Trophic ecology of a blooming jellyfish (Aurelia coerulea) in a Mediterranean coastal lagoon

Raquel Marques, Delphine Bonnet, Claire Carré, Cécile Roques, Audrey M.
Darnaude

Trophic ecology of a blooming jellyfish (*Aurelia coerulea*) in a Mediterranean coastal lagoon

Raquel MARQUES[1], Delphine BONNET[1], Claire CARRÉ[1], Cécile ROQUES[1], Audrey M. DARNAUDE[1]

[1] MARBEC, Univ. Montpellier, CNRS, Ifremer, IRD, Montpellier, France

Corresponding author:

marques.rfs@gmail.com / raquel.marques@umontpellier.fr

CC093, Place Eugène Bataillon, 34095 Montpellier Cedex 05, France

Tel: +33769370312

Co-authors contact:

delphine.bonnet@umontpellier.fr; claire.carre@ird.fr; Cecile.Roques@cnrs.fr;

Audrey.Darnaude@cnrs.fr

Running head: Trophic ecology of jellyfish in a coastal lagoon

Key words: Stable Isotopes, Diet, Trophic niche, Trophic competition, Population dynamics, Scyphistomae, Medusae, Oysters

Abstract

The current lack of knowledge on the trophic ecology of scyphozoans, particularly at the benthic stage, prevents a full understanding of the controls on many jellyfish blooms. The blooming scyphozoan (*Aurelia coerulea*) completes its entire life cycle in the Thau lagoon (southern France), where the annual population dynamics of both its benthic and pelagic stages have been described. This offered an exceptional framework to investigate the trophic processes regulating jellyfish populations over time. To this aim, stable isotopic signature analysis ($\delta^{13}C$ and $\delta^{15}N$) was used to infer the diet of both *A. coerulea* scyphistomae and medusae over one year. These results were matched with medusae gut content analysis and with the monthly abundances of local plankton groups. Lastly, the isotopic signatures of *A. coerulea* scyphistomae and medusae were compared with those of the oysters (*Crassostrea gigas*) cultivated in the lagoon to evaluate the potential interspecific trophic competition. The results revealed two seasonal shifts in the trophic niche of *A. coerulea* and substantial overlap between the diets of its benthic and pelagic stages. Conversely, trophic niche overlaps with the oysters were restricted, suggesting a limited impact of the local jellyfish bloom on shellfish production. Phytoplankton, microzooplankton, mesozooplankton, and sedimentary organic matter were all important food sources during critical periods of *A. coerulea* life-cycle. However, microzooplankton abundance was found to be key for the production of buds by the scyphistomae and, therefore it is likely to control the benthic population size and, thereby, to modulate the intensity of its annual bloom in Thau.

Introduction

Due to the impact of their conspicuous blooms on coastal ecosystems functioning and economic activities, jellyfish have received increasing scientific attention during the last decades (Purcell 2012). In particular, the ecological drivers of jellyfish mass occurrences have been investigated, revealing a complex interaction of natural (e.g. Condon et al. 2012) and anthropogenic (e.g. Purcell 2012) causes. However, uncovering the drivers of blooms is particularly challenging for most scyphozoan blooming species because their life-cycle comprises a benthic (scyphistomae) and a pelagic (ephyrae and medusae) phase (e.g. Lucas 2001). Therefore, bloom formation is a joint consequence of the production of pelagic ephyrae by the benthic scyphistomae and of their survival and growth into medusae. As a result, the ecology of both life stages controls bloom intensity.

Bottom-up processes within food webs often play a key role in ecological systems functioning and are amongst the most important drivers of jellyfish blooms (Boero et al. 2008). Food quality and availability are known to control the production of ephyrae by the scyphistomae (Han and Uye 2010; Ikeda et al. 2017) and to modulate the growth rate of medusae (Ishii and Båmstedt 1998). This supports the need for comprehensive studies on the trophic ecology of both life stages in the field. Yet, although information is growing on the trophic ecology of medusae (e.g. Javidpour et al. 2016; Milisenda et al. 2018), the diet of jellyfish scyphistomae is still poorly known.

Jellyfish from the *Aurelia* genus are present globally in coastal areas and are among the most common scyphozoans that form blooms (Mills 2001). Large accumulations of *Aurelia* spp. have been reported all around the world, including in the Mediterranean, where they occur mainly in protected waters and semi-enclosed seas (Mills 2001). Their medusae have been described as zooplanktivorous, with a dominance of mesozooplankton, especially copepods, in their diet (e.g. Ishii and Tanaka 2001; Lo and Chen 2008). However, while

3

65 microzooplankton and benthic food sources have been considered for long as negligible food

66 sources for jellyfish, recent findings based on new techniques (such as stable isotope analysis)

67 suggest the opposite (Javidpour et al. 2016). In laboratory studies, newly hatched *Artemia* sp.

68 are usually provided as food (e.g. Han and Uye 2010, Hubot et al. 2017), but the few studies

69 regarding the diet of *Aurelia* sp. scyphistomae in the wild suggest that they eat a mix of

70 phytoplankton (Huang et al. 2015), microzooplankton (Kamiyama 2013) and small

71 mesozooplankton species (e.g. copepods, cladocerans, gelatinous zooplankton; Östman 1997).

72 Considering the critical role of scyphistomae in the formation of scyphozoans blooms, it is

73 urgent to specify natural prey preferences in *Aurelia* species and the potential trophic

74 competition among their benthic and pelagic stages to understand blooms formation in this

75 genus and evaluate their ecological consequences.

76 Situated along the North-western Mediterranean coast, the Thau lagoon offered an

77 exceptional framework for this. Indeed, this lagoon presents the rare particularity to harbour a

78 complete resident population of *Aurelia coerulea* (Bonnet et al. 2012; Marques et al. 2015a),

79 which allows investigating the trophic processes that regulate its population dynamics at both

80 stages. The scyphistomae of *A. coerulea* are widespread in the lagoon, fixed mainly on

81 biofouling organisms that grow on anthropogenic structures (predominantly on oysters and

82 mussels; Marques et al. 2015a). They are present all year round, with a peak of coverage in

83 the Spring (April) and lower densities in the Summer and Autumn (Marques et al. 2019).

84 Ephyrae appear in the early winter (November – December) and give rise to adult medusae at

85 the beginning of the Spring (April – May), generating the annual jellyfish bloom, which

86 persists until June – July (Bonnet et al. 2012; Marques et al. 2015b). Because no clear link

87 was found between the abundance of mesozooplankton in the lagoon and the benthic

88 population dynamics of *A. coerulea*, it was suggested that other food sources might sustain

89   the species local production (Marques et al. 2019). Nevertheless, further confirmation is still

90   required in this regard.

91   Coastal lagoons are usually very productive environments, where high continental inputs in

92   nutrients and particulate organic matter sustain high and diversified primary and secondary

93   productions (Nixon et al. 1995). This benefits the whole food web and enhances the growth of

94   lagoon predators like juvenile fish (Escalas et al. 2015). In Thau, it also supports a massive

95   shellfish production: ~10% of the Pacific oysters *Crassostrea gigas* produced in France come

96   from the lagoon, with a yearly shellfish production of 15 000 tons (Mongruel et al. 2013).

97   In this context, the present work not only aimed to describe the trophic ecology of both the

98   benthic and the pelagic life-stages of *A. coerulea* in Thau and assess its influence on critical

99   periods of population dynamics of this jellyfish (e.g. peak of bud production, strobilation, and

100   medusae growth), but also to evaluate whether *A. coerulea* medusae and scyphistomae

101   compete for food with the Pacific oysters reared in the lagoon. For this, we combined

102   medusae gut content assessments with stable isotopes analysis. This latter technique has been

103   increasingly used to study the structure and transfer of organic matter within coastal food

104   webs (Layman et al. 2012) and has recently allowed uncovering the diet, trophic levels, and

105   trophic interactions of different jellyfish species (Fleming et al. 2015; Javidpour et al. 2016;

106   Milisenda et al. 2018). Using it to explore the changes in *A. coerulea* diet during a full annual

107   cycle should allow assessing whether its benthic and pelagic stages occupy the same trophic

108   niche than the oysters cultivated in the lagoon. This strongly contributes to a better

109   understanding of the impacts of *A. coerulea* blooms on the local shellfish production.

110

111   **Material and Methods**

112   *Study site*

113   The Thau lagoon is a semi-enclosed marine coastal lagoon of 75 km^2 area, connected

114   to the Mediterranean Sea by three narrow channels (Fig. 1). It is relatively shallow, with mean

115   and maximum depths of 4 and 10 m, respectively (except for a localized depression of 24 m).

116   The local tidal range (< 1m) is weak, so water residence time in the lagoon is globally high

117   (1–-4 months) and strongly influenced by seasonal strong wind events (Millet and Cecchi

118   1992). The lagoon environment parameters show strong seasonal variations, characteristic of

119   temperate regions, with temperature and salinity at their lowest in the winter (with minimum

120   values of 7.6 and 35.0, respectively) and at their highest in the summer (with maximum

121   values of 25.8 ℃ and 39.6, respectively; Marques et al 2019). The lagoon mainly receives

122   water from the Sète canal that connects it to the Mediterranean Sea and from several small

123   intermittent rivers that drain its catchment area (290 km^2, Plus et al. 2006). These later dry out

124   between May and September and show occasional flash floods in the wet season (Fouilland et

125   al. 2012). As a result, marine conditions prevail in the lagoon, the annual influence of the

126   freshwater coming from the watershed being highly dependent on the intensity of rainfall

127   events during the winter (Plus et al. 2006). With regards to anthropogenic influence, the

128   lagoon is under multiple pressures due to the presence of the touristic city of Sète and many

129   small villages and agriculture fields on its coastline. Shellfish farming is the most important

130   economic activity on the lagoon (Mongruel et al. 2013): around 20% of its surface is occupied

131   by farms, mainly in the northern and north-western parts (Fig. 1).

132

133   *Sampling*

134   For this study, the jellyfish and their potential food sources were sampled in the

135   eastern part of the lagoon, at two close sites where the benthic and the pelagic population

136   dynamics of *A. coerulea* had been previously described (Bonnet et al. 2012; Marques et al.

137   2015b; Marques et al. 2019). Both sites (benthic sampling site: 43°25'31.1"N; 03°42'0.9"E

6

138   and pelagic sampling site: 43º23'59.1''N; 03º36'37.2''E; Fig. 1) are located on soft-bottom

139   sediments punctuated by sparse seagrass meadows and are strongly influenced by marine

140   water influxes due to their proximity to the Sète channel, which connects the lagoon to the

141   Mediterranean Sea.

142   *A. coerulea* scyphistomae were collected monthly on a partially submerged boat present at

143   the benthic sampling site (see Marques et al. 2019 for more details), over an entire calendar

144   year (from January 2017 to January 2018). For this, mussel shells with sizeable aggregates of

145   scyphistomae attached on their underside surface (three per sampling date) were collected

146   directly on the surface of the boat by SCUBA diving. They were brought to the laboratory in

147   ambient water and placed in 0.2-µm-filtered seawater (ca. 20ºC) for about 2h to ensure all

148   scyphistomae had empty guts. Fifty individual scyphistomae were then collected under a

149   dissecting microscope (Olympus SZ40; Olympus KL 1500 LCD), using needles and tweezers

150   to carefully detach them, and preserved in cryotubes at –30ºC.

151   The pelagic ephyrae of *A. coerulea* are usually present in the lagoon from November to April

152   (Bonnet et al. 2012; Marques et al. 2015b). However, because stable isotope analysis requires

153   pooling high numbers of these small organisms to be applicable, sampling for this life stage in

154   this work was successful in January 2018 only. The ephyrae were collected near the water

155   surface at the pelagic sampling site, by horizontal towing, using a modified WP2 plankton net

156   (1.2 m long, 50-cm opening, and 200-µm mesh). In the laboratory, they were picked and kept

157   for ca. 2h in filtered seawater to allow for complete gut evacuation. Then 50 individuals were

158   pooled per sample and preserved at –30ºC.

159   *A. coerulea* medusae (i.e., pelagic individuals with bell diameter > 1 cm), were collected

160   every two weeks at the pelagic sampling site, from March to June 2017, i.e., over the entire

161   period of their presence in the lagoon. They were collected in surface waters using hand nets

162   and transported to the laboratory in ambient water. Five individual medusae were then

163 randomly selected and prepared for stomach content analysis. For this, they were each

164 partially dried on a paper towel to remove excess water, measured (bell diameter in cm),

165 weighted (total wet weight in g), and individually preserved in 4% buffered formaldehyde.

166 The remaining medusae were kept for ca. 2h in 0.2 µm filtered seawater (ca. 20ºC) to empty

167 their guts. Three of them were then placed on a paper towel for about 1 minute (30 s on each

168 side) to remove excess water, weighed, and measured. As bell tissue is the most suitable body

169 part for stable isotope analysis in jellyfish (D'Ambra et al. 2014), gonads, oral arms, and

170 gastric pouches were removed from each medusa. The remaining individual bell tissues were

171 preserved separately at -30ºC. In March 2017, due to the small size of the medusae (ca. 2 cm

172 bell diameter), eight complete individuals were pooled per replicate before preservation at -

173 30ºC.

174 For this work both the plankton and the sedimentary organic matter of the lagoon were also

175 sampled as they both constitute potential food sources for *A. coerulea*. Samples for these two

176 components were collected at pelagic and benthic sampling sites, respectively, on the same

177 sampling dates as *A. coerulea* medusae and scyphistomae collection. Within the plankton, the

178 fraction larger than 200 µm, that between 60 and 200 µm and that between 20 and 60 µm

179 were assumed to be composed mainly by mesozooplankton, microzooplankton, and

180 phytoplankton, respectively. Mesozooplankton samples were collected near the surface, by

181 horizontal towing, using a modified WP2 plankton net (length: 1.2 m; opening area: 50 cm;

182 mesh size: 200 µm). Once in the laboratory, each sample was filtered through a 60 µm mesh

183 sieve to eliminate excess water and divided into five subsamples. Microzooplankton and

184 phytoplankton samples were also collected by horizontal towing near the surface, but using a

185 phytoplankton net (length: 1 m; opening area: 30 cm; mesh size: 20 µm). Once in the

186 laboratory, each sample was filtered through a 200-µm sieve. The size fraction > 200 µm was

187 discarded. The remaining sample was then separated into the two size fractions,

188 corresponding to microzooplankton and phytoplankton, using a 60 μm sieve, and then divided

189 into 5 subsamples. For each plankton size fraction, the subsamples were collected separately

190 on pre-combusted (500ºC for 24h) Whatman GF/F filters. Two filters of each plankton

191 component were acidified with 1% HCl and triple rinsed with distilled water to remove

192 inorganic carbon, which can bias C stable isotope results (Yokoyama et al. 2005). The

193 remaining non-acidified filters were used for N stable isotope analysis, since sample

194 acidification may affect the stable isotope signature for this element (Pinnegar and Polunin

195 1999). All samples were preserved at –30ºC until further analysis. For sedimentary organic

196 matter, the first 2 cm of the sediment were collected by SCUBA diving at the benthic

197 monitoring site. Samples (2 replicates) were carefully scrutinized to eliminate any large

198 organisms, sediment inorganic particles, or vegetal debris, before preservation at –30ºC.

199 To investigate the trophic interactions between *A. coerulea* and the local oysters, both wild

200 and cultivated individuals of *Crassostrea gigas* were sampled seasonally from October 2017

201 to August 2018, including during the peak of the jellyfish bloom (which occurred in June in

202 2018). Wild oysters (mean size: 11.5 ± 2.0 cm) were collected by SCUBA diving at the

203 benthic monitoring site, while the cultivated ones (mean size: 11.9 ± 1.0 cm) were obtained

204 from the shellfish producer *Huitres-Bouzigues.com*. Immediately after their removal from the

205 lagoon, the oysters were transported to the laboratory in ambient water, measured and

206 carefully dissected to collect their adductor muscle. The muscle tissues were then rinsed with

207 distilled water and preserved separately at –30ºC until further analysis.

208

209 *In situ abundance of plankton in the Thau lagoon*

210 Phytoplankton, microzooplankton and mesozooplankton samples were collected at the pelagic

211 monitoring site, every two weeks from January to June 2017 and monthly onwards, until

212 December 2017. For phytoplankton, 10 to 20L of surface water were collected, filtered with a

213   15-µm-mesh net, and preserved with 2% buffered formaldehyde. For microzooplankton, a

214   subsample of 30 ml of surface water was preserved with 2% buffered formaldehyde (to

215   estimate ciliates' abundance) and one of 110 ml was preserved with Lugol's solution (to

216   estimate heterotrophic flagellates' abundance). Phytoplankton and microzooplankton species

217   were identified and counted using sedimentation chambers and an inverted microscope

218   (Olympus IX70) following the Utermöhl method (Utermöhl 1958). Mesozooplankton samples

219   were collected near the surface by horizontal towing using a modified WP2 plankton net (1.2

220   m long, 50-cm opening, and 200-µm mesh). Samples were immediately preserved in 4%

221   buffered formaldehyde until further analysis in the laboratory. Mesozooplankton abundance

222   was determined by counting organisms under a dissecting microscope (Olympus SZX7 –

223   ILLT). The diversity of mesozooplankton was not assessed.

224

225   *Gut content analyses*

226   To evaluate the diet of *A. coerulea* medusae, their gastric pouches, oral arms, and the

227   preserving solution were examined under a dissecting microscope (Olympus SZX7 – ILLT).

228   Although *A. coerulea* medusae were present in the lagoon from March, most individuals

229   exhibited empty guts during this month. Therefore, gut content analysis was only performed

230   on the medusae collected between April and June. For this, only complete exoskeletons were

231   considered for prey identification. This was done to the lowest possible taxonomic level,

232   although the level of exoskeleton digestion often precluded prey identification down to the

233   species level. The importance of each prey in the diet was expressed by the following indices:

234   (i) the frequency of occurrence (in %), which represents the percentage of medusae with the

235   prey *i* in their guts among all those that had non-empty guts; (ii) the index of relative

236   importance (in %), representing the percentage of prey *i* in relation to the total number of prey

237 items found in the non-empty guts; and (iii) the mean abundance of prey i in non-empty guts

238 (in ind. medusae^{-1}).

239

240 *Stable isotope analysis*

241 All filters containing plankton (phytoplankton, microzooplankton, and mesozooplankton)

242 were oven-dried at 60ºC for 48h and the biological material was gently scraped off the filter

243 surface. Samples for the sedimentary organic matter, the oysters, *A. coerulea* medusae,

244 scyphistomae, and ephyrae were freeze-dried for 48h and ground to a fine powder using a

245 mortar and pestle. The sedimentary organic matter samples were divided into two subsamples.

246 One half was used directly for N stable isotope analysis. The remaining subsample was

247 acidified with 1% HCl to remove carbonates before C stable isotope analysis, rinsed several

248 times with distilled water, and oven-dried at 70ºC.

249 Stable isotopic analyses for biological samples were performed using a PDZ Europa ANCA-

250 GSL elemental analyser interfaced with a PDZ Europa 20-20 isotope ratio mass spectrometer

251 (Sercon Ltd., Cheshire, UK). Measurements of $\delta^{13}C$ and $\delta^{15}N$ signatures were performed each

252 on 1.5 to 4 mg of dry samples, with exception of the medusae, for which ca. 10 mg of dry

253 sample was required for successful analysis, after salt content correction, based on dry weight

254 and ash-free dry weight relationships (Lucas et al. 1994; Pitt et al. 2009). Sedimentary organic

255 matter samples (of ca. 55 mg each) were analysed using an Elementar Vario EL Cube or

256 Micro Cube elemental analyser (Elementar Analysensysteme GmbH, Hanau, Germany)

257 interfaced to a PDZ Europa 20-20 isotope ratio mass spectrometer (Sercon Ltd., Cheshire,

258 UK). Calibration was performed against NIST Standard Reference Materials (IAEA-600,

259 USGS-40, USGS-41, USGS-42, USGS-43, USGS-61, USGS-64, and USGS-65). Isotope

260 ratios of all samples were expressed as parts per thousand (‰) differences from the internal

261   reference standards (glutamic acid, alfalfa flour, nylon 6, bovine liver, and enriched alanine)

262   using the following equation:

263     $$\delta X = \left[\left(\frac{R_{sample}}{R_{standard}}\right) - 1\right] \times 1000$$

264   where X is the ^{13}C or ^{15}N and R is the corresponding ratio, ^{13}C/^{12}C or ^{15}N/^{14}N.

265   As the lipid content of organisms affects their δ^{13}C signatures, δ^{13}C correction is required

266   when C:N is higher than 3.5 (Post et al. 2007). Therefore, the δ^{13}C values obtained for *A.*

267   *coerulea* scyphistomae and medusae (mean C:N 3.7 ± 0.1 and 3.9 ± 0.6, respectively) and for

268   the mesozooplankton (mean C:N of 6.9 ± 3.0) were corrected (δ^{13}C$_{corr}$) according to the

269   equations proposed by D'Ambra et al. (2014) for jellyfish:

270     $$\delta^{13}C_{corr} = \delta^{13}C_{initial} - 9.43 + 2.69 \times C{:}N$$

271   and by Syväranta and Rautio (2010) for zooplankton:

272     $$\delta^{13}C_{corr} = \delta^{13}C_{initial} + 7.95 \times \left(\frac{C{:}N - 3.8}{C{:}N}\right)$$

273

274

275   *Relationship between benthic population dynamics and plankton abundance*

276   Data on *A. coerulea* benthic population dynamics were obtained from Marques et al. (2019).

277   Generalized linear models (using linear and logistic regressions, without interactions) were

278   employed to assess the respective contributions of the absolute abundances of the non-

279   averaged phytoplankton, the microzooplankton and the mesozooplankton (after logarithmic

280   transformation ln (x+1)) to temporal trends in the scyphistomae density (% coverage) and in

281   the proportion of the scyphistomae producing buds. The models were validated by

282   examination of residuals versus fitted values plots (Zuur et al. 2009).

283

284   *Determination of Isotopic Niche Periods*

12

285　To reveal potential shifts in the trophic niches of *A. coerulea* scyphistomae and medusae

286　during the year and identify the periods when they present unchanging isotopic signatures

287　(hereafter "Isotopic Niche Periods"), a cluster analysis was performed on the monthly mean

288　isotopic values of both life stages (Jain 2010). For this, partitioning algorithms, based on the

289　k-means clustering method, were applied using the package "factoextra" (Kassambara and

290　Mundt 2017). The k-means approach subdivides the data into a set of k groups so that the sum

291　of squares from the data points to the center of each group is minimized (Kassambara and

292　Mundt 2017). This clustering approach allowed to identify the successive isotopic niche

293　periods for both life stages, providing the basis for identifying their successive sources of

294　organic matter during the year.

295

296　*Assessment of potential intra- and interspecific trophic competition*

297　Our sampling design allowed for reliable estimation of the potential intraspecific trophic

298　competition between *A. coerulea* scyphistomae and medusae within each isotopic niche

299　period. However, because oyster and jellyfish samples were collected in different years

300　(except for one isotopic niche period), the trophic competition between the two species was

301　only investigated globally, assuming that interannual variability in the trophic niche in the two

302　species is negligible. In both cases, the Bayesian framework proposed by Jackson et al. (2011)

303　for evaluating trophic competition was used. For this, Bayesian multivariate normal

304　distributions were first fitted to the isotopic signatures of all organisms. Then, the overlap

305　between their trophic niches was calculated based on maximum likelihood fitted ellipses,

306　using the function "maxLikOverlap" from the R package "SIBER" (Jackson et al. 2011).

307

308　*Determination of jellyfish diet using Stable isotope analysis*

309   Differences in isotopic signatures (δ^{13}C and δ^{15}N) among the main local potential food

310   sources (phytoplankton, microzooplankton, mesozooplankton, and sedimentary organic

311   matter) were tested by a PERMANOVA (Anderson 2017) on the log10 transformed Bray-

312   Curtis distance matrix ($-\delta^{13}$C and δ^{15}N), made using the package "vegan" (Oksanen et al.

313   2019), followed by pairwise comparisons made using the "pairwiseAdonis" package in R

314   (Martinez Arbizu 2019). Sources with no significant differences were grouped for subsequent

315   analyses.

316   Diet compositions for *A. coerulea* scyphistomae and medusae within each isotopic niche

317   period were assessed using Bayesian mixing models developed specifically for stable isotope

318   analysis ("MixSIAR" package, Stock and Semmens 2016). By generating the probability

319   distributions of all potential mixing solutions with the associated confidence intervals (based

320   on 300 000 chain length), this approach allows identifying the most likely contribution for

321   each food source. MixSIAR further provides a graphical user interface that allows

322   investigation of the contributions of multiple food sources to the diet of target predators,

323   considering not only the isotopic signatures (δ^{13}C and δ^{15}N) of the sources and the predators

324   but also the uncertainties and variability around these estimates. Finally, the method allows us

325   to use different isotopic fractionation factors at each trophic level. As previously performed in

326   other studies on jellyfish diet (e.g. Morais et al. 2017), the fractionation values applied here

327   for both *A. coerulea* life stages were those proposed by Vander Zanden and Rasmussen

328   (2001): for δ^{13}C we used 0.47 ± 1.23 ‰ in all cases, while for δ^{15}N we used 2.52 ± 2.5 ‰ and

329   3.23 ± 0.41 ‰ according to the type of food consumed (plant vs. animal, respectively). Like

330   Fleming et al. (2015) and Milisenda et al. (2018), we did not use the fractionation values

331   reported by D'Ambra et al. (2014), since they are very distinct from those mostly used in the

332   literature (Vander Zanden and Rasmussen 2001; Post 2002) and they still require further

333   laboratory corroboration (D'Ambra et al. 2014).

334   The basal tissue turnover rate for *Aurelia* sp. is of ca. 1 ‰ day^{-1} for $\delta^{13}C$ and 2‰ day^{-1} for

335    $\delta^{15}N$, and it takes 18 to 20 days for the tissues of this jellyfish to reach the stable isotopic

336   equilibrium with the food ingested (D'Ambra et al. 2014). To account for such turnover rates,

337   MixSIAR models were run by isotopic niche period, but jellyfish signatures at a given

338   sampling date were matched with those recorded one month earlier for all potential food

339   sources.

340

341   **Results**

342   *Medusae gut contents*

343   Among the 25 medusae collected for gut content analysis from April to June 2017, 21 had

344   food in their guts. The bell diameter of these individuals did not vary significantly over time

345   (ANOVA, $F_2 = 1.4$, p-value = 0.2), remaining at ca. 8.5 cm. Overall, gut content composition

346   predominantly consisted of mesozooplankton (>88%). Microzooplankton (mainly tintinnids)

347   and phytoplankton (mainly diatoms and dinoflagellates) represented only 8 and 4% of the

348   total prey identified, respectively, and they were only found in the guts in April and May (Fig.

349   2, Table 1, Supplementary Table 1). In April, phytoplankton and microzooplankton occurred

350   in 20 and 60% of the guts analysed, but their relative importance and abundances were still

351   low (< 7.5% and < 2.2 ind.medusa^{-1}, respectively, Table 1). In May, frequency of occurrence

352   increased for phytoplankton (33%) and slightly decreased for microzooplankton (56%) and

353   showed a growing trend of their relative importance for both groups (5.6 and 12.5%,

354   respectively, Fig. 2). Indeed, in May, microzooplankton relative importance was higher than

355   some mesozooplankton organisms, like the "other crustaceans" group, which includes

356   cladocerans and ostracods (10.0%; Table 1, Supplementary Table 1). Masses of unidentified

357   organic matter were also recurrently observed over the entire study period.

358   Twenty-four different taxa of mesozooplankton were identified in the guts of the medusae,

359   but, among them, copepods and nauplii (from cirripeds and copepods) dominated. They

360   occurred in 40 to 88.9% of the guts analysed and represented up to 46.3% of the prey

361   identified (in June, Table 1). The maximum average abundance of mesozooplankton

362   organisms in the guts (26.2 ± 35.4 ind.medusae^{-1}) was recorded in April when non-crustacean

363   taxa (mainly gastropod veliger), and copepods represented more than 80% of the prey

364   identified in medusae gut contents (Table 1). Nauplii (index of relative importance = 31.3%)

365   were the most important mesozooplanktonic prey in the guts in May, while in June, copepods

366   dominated (index of relative importance = 46.3%, Table1).

367

368   *Prey availability and relationship with benthic population dynamics*

369   Prey abundances in *A. coerulea* medusae gut contents did not reflect their availability in the

370   water column. The abundances of phytoplankton, microzooplankton, and mesozooplankton in

371   the lagoon all showed high intra-annual variability (Fig. 3), with respective peaks in January

372   (25 138 ± 34 047 cell.L^{-1}) and May (35 794 ± 18 374 and cell.L^{-1}), in February, April, and

373   September (> 6 200 cell.L^{-1}) and in June (90 895 ± 107 072 ind.m^{-3}). Thus, when *A. coerulea*

374   medusae were present in the water column, the planktonic community was mainly dominated

375   by phytoplankton in April and May, and by mesozooplankton in March and June, while the

376   microzooplankton showed consistently lower abundances despite a small peak in April. In

377   terms of species composition, the most abundant phytoplanktonic and microzooplanktonic

378   taxa in the water column during the study period were *Chaetoceros* sp. and *Strombidium* sp.,

379   respectively (Supplementary Table 2). Mesozooplankton diversity was not assessed, but

380   *Acartia* sp. are recurrently the most abundant taxa in Thau (Boyer et al. 2013).

381   Annual variations in scyphistomae coverage, which peaked in April (11.6 ± 3.7 %, Marques

382   et al. 2019), were positively correlated with the non-averaged abundance of phytoplankton

383   (Generalized linear models, t-value = 2.97, p-value = 0.01, Table 2, Fig. 4). In turn,

384   fluctuations in the mean percentage of scyphistomae producing buds, which varied between

385   0.4 ± 0.7 % in November and 25.2 ± 7.3 % in September (Marques et al. 2019, Fig. 4), were

386   positively correlated with variations in non-averaged microzooplankton abundance

387   (Generalized linear models, t-value = 10.19, p-value < 0.01, Table 2).

388

389   *Temporal variation of A. coerulea isotopic signatures*

390    $\delta^{13}C$ and $\delta^{15}N$ signatures showed significant temporal variation for both the scyphistomae and

391   medusae (one-way PERMANOVA, Pseudo-F_{11} = 22.7, p-value < 0.01 and Pseudo-F_3 = 38.6,

392   p-value = 0.001, respectively), but differences between life stages were never significant

393   during the period of medusae presence, from March to June (one-way PERMANOVA,

394   Pseudo-F_1 = 1, p-value = 0.4). The mean bell diameter of the medusae used for stable isotope

395   analysis, showed a sharp increase between March (1.0 ± 0.3 cm) and June (8.9 ± 1.1 cm), with

396   an estimated overall growth of 0.8 mm.day^{-1}. Over this period, medusae $\delta^{13}C$ signatures

397   increased progressively from –23.4 ± 0.1‰ to –19.4 ± 0.5‰, while their $\delta^{15}N$ signatures

398   remained stable for the first three months (at ca. 8.1‰), and increased (to a maximum at 8.9 ±

399   0.3‰) only in June (Fig. 5). For the scyphistomae, minimum $\delta^{13}C$ values were registered at

400   the beginning of the study period (in January 2017, mean: –23.4 ± 0.1‰). The $\delta^{13}C$ signatures

401   then increased to reach maximum values in June, July, and August (> –19.4‰) before

402   decreasing again until January 2018 (–22.3 ± 0.4‰). The $\delta^{15}N$ signatures of scyphistomae

403   showed a similar temporal trend, with low values at the beginning and the end of the study

404   period (8.3 ± 0.1‰ and 8.0 ± 0.4‰ in January 2017 and 2018, respectively), and maximum

405   values in July and August (>9‰). The minimum values of $\delta^{15}N$ signatures, though, were

406   observed in February 2017 (7.1 ± 0.5‰). The average $\delta^{13}C$ and $\delta^{15}N$ signatures of the ephyrae

407   collected in January 2018 (bell diameter of 0.21 ± 0.1 cm) were of –22.8 ± 0.1‰ and 8.5 ±

408   0.3‰, respectively. They did not differ significantly from those of the scyphistomae collected

409   at the same sampling time (T-test, t = –1.9, df = 2.3 p-value = 0.2 and t =1.2, df = 2.6, p-value

410   = 0.3, for δ^{13}C and δ^{15}N respectively).

411   The clustering analysis revealed three distinct groups of isotopic signatures among the

412   monthly values obtained for all life stages of *A. coerulea* (Fig. 6) allowing to identify three

413   isotopic niche periods during the year.: Period 1 gathered the δ^{13}C and δ^{15}N signatures of all

414   life stages from December to April, irrespective of the year (2017 or 2018). Period 2 reflected

415   the signatures of both the medusae and the scyphistomae from June to August. Period 3

416   corresponded to the signatures of the scyphistomae from September to November, together

417   with the signatures of the medusae and the scyphistomae in May. However, May showed a

418   particular sharp shift in δ^{13}C and δ^{15}N reflecting the rapid transition from the isotopic

419   signature of period 1 to that of period 2 and, therefore, it was not included in any isotopic

420   niche period.

421

422   *Monthly variability of organic matter sources signatures*

423   δ^{13}C and δ^{15}N signatures varied significantly according to the organic matter source and the

424   month (significant interaction, PERMANOVA, *Pseudo-F*$_{17}$ = 23.1, p-value < 0.01; Fig. 7).

425   For carbon signatures, minimum δ^{13}C values for phytoplankton, microzooplankton and

426   mesozooplankton (of –24.7 ± 0.3, –23.3 ± 0.1 and –23.7 ± 0.0 ‰, respectively) were all

427   observed in March. A sharp increase in δ^{13}C was observed in the following months, with

428   maximums in May for mesozooplankton (–18.8 ± 0.2 ‰) and in November for phytoplankton

429   (–19.0 ± 0.0 ‰) and microzooplankton (19.9 ± 0.1 ‰). Concerning nitrogen signatures,

430   mesozooplankton was the organic matter source with the highest δ^{15}N values, ranging from

431   7.3 ± 0.3 (in May) to 8.4 ± 0.0‰ (in March). Minimum δ^{15}N values were also observed in

432   May for the phytoplankton and the microzooplankton (at 5.8 ± 0.5 ‰ and 6.0 ± 0.3 ‰,

respectively) but, for these two organic matter sources, maximum values were observed in July (at 6.7 ± 0.3 ‰ and 7.4 ± 0.2 ‰, respectively). Moreover, another peak in $\delta^{15}N$ (at 6.7 ± 0.0 ‰) was observed in February for the phytoplankton. For the sedimentary organic matter, both the $\delta^{13}C$ and $\delta^{15}N$ signatures decreased from March (–18.9‰ and 5.8‰, respectively) to April (–20.7‰ and 5.5‰, respectively), remaining constant afterwards.

Contribution of organic matter sources to A. coerulea isotopic signatures

Since the $\delta^{13}C$ and $\delta^{15}N$ signatures of the phytoplankton and the microzooplankton were not significantly different (PERMANOVA post-hoc test, Pseudo-F_1 = 5.7, adjusted p-value = 0.17) these two organic matter sources were pooled as Small Plankton group in the mixing models used to assess the diet of *A. coerulea*. The remaining sources were included individually in the models (Table 3). The contribution of each source was found to vary according to the isotopic niche periods and the life stage of *A. coerulea* considered (Fig. 8). For the scyphistomae, the model suggested a dietary shift from small plankton consumption in period 1 (93.3%) to a diet based on a mix of benthic (36.6% of sedimentary organic matter) and pelagic (39.3% of mesozooplankton and 24.4% of small plankton) sources in period 2. The same occurred in period 3, although the small plankton was the main food source (69.2%), and sedimentary organic matter contribution decreased (27.0%). For the medusae, small plankton was the only food source (100%) in period 1, but the diet changed in period 2, including mainly sedimentary organic matter (64.3%) and mesozooplankton (32.3%). As the isotopic signatures of the ephyrae collected in January 2018 were very similar to those of the scyphistomae in the same period, their diet probably mainly consist of small plankton organisms.

Intra- and interspecific competitions for the food resources

458   Intraspecific isotopic niche overlap was substantial during the whole period of co-occurrence

459   of the benthic and pelagic stages of *A. coerulea* in the lagoon (March to June; Fig. 9). Indeed,

460   although the percentage of niche overlap was higher in period 1 (41.5%) than in period 2

461   (only 9.9%), the isotopic niche of the medusae entirely overlaid that of the scyphistomae in

462   period 2. Similarly, although only three ephyrae samples were analysed in this study (all from

463   January 2018), their isotopic signatures were close to those observed for the scyphistomae in

464   period 1, suggesting high (although not quantifiable) trophic niche overlap among these two

465   life stages.

466   In Thau, interspecific trophic competition between *A. coerulea* and bivalves was observed,

467   although limited. The δ^{13}C and δ^{15}N signatures of the oysters from the lagoon varied from –

468   25.6 to –18.5 ‰ and from 8.4 to 9.4‰, respectively (Fig. 10). Significant differences in

469   isotopic signatures were observed between cultivated and wild individuals (PERMANOVA,

470   Pseudo-F_{11} = 12.4, p-value < 0.01; Fig. 10), with the former showing significantly higher δ^{13}C

471   (–19.7 ± 0.9 ‰) and lower δ^{15}N (8.6 ± 0.3 ‰) signatures on average than the later (–20.1 ±

472   0.4 ‰ and 9.2 ± 0.3 ‰, respectively). Interspecific isotopic niche overlaps were limited

473   (<30%) and lower than that between cultivated and wild oysters (35.4%). Interspecific

474   isotopic niche overlap was more important between cultivated oysters and *A. coerulea* medusa

475   stage (29.1%). However, if we assume that the seasonal shifts in isotopic signatures are

476   consistent among years for both the jellyfish and the oysters, the trophic competition for food

477   should only occur at a limited period of the year and only with the medusae stage. Indeed,

478   only the signatures recorded in period 2 were responsible for the interspecific niche overlap

479   observed among *A. coerulea* medusae and cultivated (21.8%) or wild (21.1%) oysters.

480

481   **Discussion**

482   To our knowledge, this is the first study to investigate the trophic ecology of both the benthic

483   and the pelagic stages of a jellyfish species (*A. coerulea*) in association with its in situ

484   population dynamics and the plankton availability. The results obtained offer the

485   unprecedented opportunity to identify the bottom-up processes regulating *A. coerulea*

486   populations, contributing to our understanding of the formation of its blooms.

487

488   *Trophic ecology of the pelagic stages of A. coerulea*

489   Ephyrae were only collected once during the study period and their isotopic signature was

490   similar to that of scyphistomae at the same time, indicating major importance of the small

491   planktonic organic matter (i.e. phytoplankton and microzooplankton) in their diet. This result

492   will have to be confirmed because, in Thau, *A. coerulea* ephyrae are mainly released in

493   November, but strobilation continues until April (Marques et al. 2019). Therefore, we cannot

494   exclude that the ephyrae caught in January 2018 had been released just a few days or weeks

495   before their collection and therefore still had the isotopic signature of the scyphistomae that

496   produced them. Moreover, because of their very low growth rate during the winter (< 0.1

497   mm.day^{-1}, Marques et al. 2015b), the ephyrae caught in January might not have yet

498   incorporated the signature of the prey ingested after their release (Frazer et al. 1997).

499   Nevertheless, phytoplankton, microzooplankton (such as rotifers) and suspended particulate

500   organic matter have all been previously identified as important food sources for ephyrae

501   (Båmstedt et al. 2001; Zheng et al. 2015) so our findings are in agreement with the literature.

502   The results from medusae gut contents analysis support previous reports describing *A.*

503   *coerulea* medusae as mesozooplanktivorous, feeding mainly on copepods and nauplii (mainly

504   of cirripeds). Indeed, *Aurelia* spp. medusae have been suggested to prey mainly on

505   mesozooplankton and to have higher clearance rates and selective preferences for crustacean

506   prey such as copepods, cirriped nauplii, and cladocerans (Hansson 2006; Lo and Chen 2008).

507   Phytoplankton and microzooplankton also contributed to the diet of *A. coerulea* medusae in

508   Thau, but only during their first two months of growth and with low relative importance.

509   Indeed, *Aurelia* spp. diet often echoes prey local abundances in their environment (e.g. Ishii

510   and Tanaka 2001), which might explain these results, since the abundance of

511   microzooplankton and phytoplankton in the lagoon were higher in April and May. Yet,

512   variations of prey availability in Thau were not entirely reflected in *A. coerulea* medusae diet,

513   since mesozooplankton represented consistently more than 80% of the prey identified in their

514   guts, despite its lower in situ abundance in this period. Although gut content analyses

515   provided important qualitative information on the diet of jellyfish medusae, conclusions

516   regarding the importance of each prey type for their growth, at longer time scales, should be

517   drawn with caution, due to the bias associated with this technique. The digestion time of

518   mesozooplankton in the medusae guts might vary between 1 and 5h, depending on medusa

519   size, temperature, and prey type (Ishii and Tanaka 2001; Martinussen and Båmstedt 2001),

520   with smaller prey being digested faster (Martinussen and Båmstedt 2001). Therefore, gut

521   content analysis often leads to an overestimation of the importance of hard and big prey in the

522   diet, such as crustaceans. This might have contributed to a general overlook of the potential

523   relevance of the lower trophic levels to the diet of jellyfish (Javidpour et al. 2016). Indeed, in

524   Thau, the diet composition of *A. coerulea* medusae differed between gut content and stable

525   isotope analyses. The later approach underlined not only the importance of the phytoplankton

526   and microzooplankton (pooled as small plankton) for the diet of *A. coerulea* medusae in Thau

527   but also that of the sedimentary organic matter.

528   The diet of the *A. coerulea* medusae varied over time. In general, the δ^{13}C (–23.4 to –19.4‰)

529   and δ^{15}N (8.1 to 8.9‰) values found for the *A. coerulea* medusae stage were in the range of

530   the values published by Fleming et al. (2015) (–20.3 to –18.1 for δ^{13}C and 8.5 to 11.8 for

531   δ^{15}N) and D'Ambra et al. (2013) (–20.5 ± 0.3‰ and 7.2 ± 0.4‰ on average for δ^{13}C and

532   δ^{15}N, respectively). However, intra-annual fluctuations in medusae isotopic signatures

533   revealed a significant shift in May, with an increase of ca. 3.5 and 1‰ for δ^{13}C and δ^{15}N,

534   respectively. This separates two distinct periods of stable isotopic signatures: period 1, during

535   medusae growth from March to April, and period 2, in June, when they reproduce before the

536   collapse of the bloom. This variation in the isotopic signature might indicate a rapid ontogenic

537   shift in the diet of the medusae, reflecting the change from small plankton to

538   mesozooplankton and sedimentary organic matter sources. A similar shift in the trophic niche

539   was also shown for *Aurelia aurita* in Northern Ireland, where medusae fed on higher trophic

540   levels by the end of their growing period (Fleming et al. 2015). Temporal variations in

541   isotopic signatures of predators might also reflect analogous changes in the isotopic signatures

542   at the base of the food webs (Post 2002). In this study, the values of the assessed organic

543   matter sources agree with those previously reported in Thau (Pernet et al. 2012) and other

544   north-western Mediterranean coastal lagoons (Dierking et al. 2012; Escalas et al. 2015) but

545   revealed significant fluctuations over time. In Thau, ^{13}C-depleted coastal inputs are dependent

546   on the rainfall, which was high in March and low in April (http://www.meteofrance.fr/climat-

547   passe-et-futur/bilans-climatiques/bilan-2017. Accessed 27 Jul 2019), likely contributing to the

548   variation in the δ^{13}C isotopic signatures of the lower trophic levels and then reflected in those

549   of *A. coerulea* medusae. However, similar trends were not observed for δ^{15}N isotopic

550   signatures, which showed a decreasing trend for most organic matter sources in May,

551   contrasting with an increasing trend for medusae in June. This underlines that the observed

552   isotopic niche shift for *A. coerulea* medusae was not only a reflection of temporal fluctuations

553   in the signatures of their prey but likely induced by a significant change in their diet. Finally,

554   our results highlight the importance of sedimentary organic matter (64.3%) in the diet of *A.*

555   *coerulea* medusae, as previously observed for *A. aurita* in the Kiel Fjord (Javidpour et al.

556   2016). Like most shallow marine ecosystems, the Thau lagoon is recurrently subjected to

557 sediment resuspension, triggered by river floods and strong wind activity (Fouilland et al.

558 2012). With this regard, the unidentified masses of organic matter found in the guts of the

559 medusae were probably aggregates of re-suspended sedimentary organic matter.

560

561 *Trophic ecology of the benthic stage of A. coerulea*

562 The temporal variability of the δ^{13}C and δ^{15}N signatures of *A. coerulea* scyphistomae

563 suggested two significant intra-annual shifts in their diet and identified three different isotopic

564 niche periods. The diet of scyphistomae was mostly based on small plankton during period 1,

565 included all available food sources during period 2 and changed to a mix of pelagic (i.e., small

566 plankton) and sedimentary organic matter during period 3. These seasonal variations agree

567 with those of the availability of planktonic food sources in the lagoon, following the high

568 abundances of phytoplankton and microzooplankton in periods 1 and 3 and that of

569 mesozooplankton in period 2 (i.e., in June). Our results agree with the few existing reports on

570 the diet of jellyfish scyphistomae, which suggested that they feed on small mesozooplankton

571 species (e.g. copepods, cladocerans, and cirripeds nauplii; Östman 1997; Ikeda et al. 2017), as

572 well as on microzooplankton and phytoplankton (dinoflagellates, ciliates, rotifers, and

573 diatoms; Kamiyama 2013; Wang et al. 2015; Huang et al. 2015). However, as for medusae,

574 the temporal variation in scyphistomae isotopic signatures might also reflect the origin of the

575 carbon and nitrogen inputs in the lagoon (Post 2002). Indeed, fluctuations in δ^{13}C and δ^{15}N

576 values might reflect the stronger contribution of terrestrial inputs to the basis of the food web,

577 after rainy events in period 1 (Vizzini et al. 2005; Pernet et al. 2012a) and the exceptionally

578 low terrestrial inputs from June onwards (periods 2 and 3), due to a very dry summer and

579 autumn in 2017 (> 80% loss of rainfall when compared with the mean between 1981 – 2010

580 in October, http://www.meteofrance.fr/climat-passe-et-futur/bilans-climatiques/bilan-2017.

581 Accessed 27 Jul 2019). Furthermore, it might also be affected by the higher influence of

582   wastewater effluent in the lagoon during dry periods (Perrin and Tournoud 2009), which is

583   suggested to induce an enrichment of $\delta^{15}N$ signatures, as in other coastal lagoons (Vizzini et

584   al. 2005; Dierking et al. 2012; Escalas et al. 2015). Yet, the skewed temporal pattern of the

585   scyphistomae isotopic signatures when compared with their sources further confirm a

586   seasonal variation in their diet.

587   The increase in mesozooplankton consumption during period 2, when the abundance of this

588   prey is maximal, is not surprising. Higher abundances of this type of prey (especially of newly

589   hatched *Artemia* sp.) is recognized to induce better performances of scyphistomae (i.e.,

590   growth, asexual reproduction, and strobilation) in laboratory experiments (e.g. Ikeda et al.

591   2017; Hubot et al. 2017). However, our results further highlight the prominent role of the

592   lower trophic levels in the feeding and benthic population dynamics of the species in Thau.

593   Although we were not able to precisely quantify the relative importance of phytoplankton and

594   microzooplankton in the diet of *A. coerulea* scyphistomae, they both appear to be important.

595   Phytoplankton cells are seemingly insufficient to support scyphistomae basic metabolic rates

596   at high temperatures (20ºC) and for long periods (Wang et al. 2015; Huang et al. 2015), but

597   they provide a suitable alternative source of energy for their survival and asexual reproduction

598   at low temperatures (Huang et al. 2015; Wang et al. 2015). Therefore, peaks in phytoplankton

599   abundances during period 1 probably support *A. coerulea* scyphistomae survival over the

600   winter and early spring. Similarly, the significant positive correlation between the abundance

601   of microzooplankton and the percentage of scyphistomae producing buds suggests that this

602   type of prey promotes the buds production, ultimately driving the benthic population density.

603   Indeed, buds production by scyphistomae of *Aurelia aurita* has been previously shown to

604   increase when reared on a ciliate-based diet rather than on the larger *Artemia* prey (Kamiyama

605   2013). Interestingly, although more buds were produced in April in the lagoon (due to high

606   scyphistomae density) the peak of the percentage of scyphistomae producing buds, as well as

607   the maximum number of buds per scyphistoma, were registered in September (Marques et al.

608   2019), co-occurring with high abundances of microzooplankton in the lagoon.

609   Lastly, as for medusae, our results highlight the importance of the sedimentary organic matter

610   in the diet of *A. coerulea* scyphistomae in Thau. This does not come as a major surprise

611   because re-suspended sediments were often observed on the scyphistomae samples collected

612   *in situ*. Sedimentary organic matter is usually composed by a mixture of microphytobenthos,

613   heterotrophic microorganisms (bacteria, ciliates, protozoans, nematodes) and detritus,

614   classically associated and re-suspended with sediment (Dubois et al. 2007), which might

615   provide a suitable source of food for jellyfish benthic stages (Östman 1997).

616

617   *Intra- and interspecific competition*

618   The benthic scyphistomae and the pelagic medusae of *A. coerulea,* although inhabiting

619   different habitats, appeared to share, at least partially, the same organic matter sources in the

620   lagoon. During period 1, their high isotopic niche overlap, and the results of the mixing

621   models, indicate that both stages feed on phytoplankton and/or microzooplankton. In period 2,

622   despite a lower isotopic niche overlap, the trophic niche of the medusae entirely covers that of

623   the scyphistomae. This suggests that during large medusae blooms and under food limitation

624   conditions, intraspecific competition for food might occur in the lagoon, with possible

625   detrimental impacts on the scyphistomae population.

626   One of the main concerns regarding the presence of *A. coerulea* in Thau is the potential

627   competition for food with the oysters produced in the lagoon, in particular during the medusae

628   blooms and due to the overspread distribution of scyphistomae (Marques et al. 2015a).

629   However, our results suggest only a limited trophic niche overlap. Although oysters and *A.*

630   *coerulea* stages were not collected in the same year (except in period 3) we assumed that the

631   isotopic signature of the oysters mostly varies intra-annually (Pernet et al. 2012). If this is

true, our results indicate that interspecific competition for food only potentially occurs

between *A. coerulea* medusae and oysters (cultivated and wild) in period 2. During this

period, sedimentary organic matter was an important source in the diet of *A. coerulea*

medusae and also reported as part of the diet of oysters (Dubois and Colombo 2014). This

might explain the isotopic niche overlap, although restricted, between these two organisms at

this period. The limited interspecific trophic competition between the *A. coerulea* and the

oysters might result from their different filtration and particle retention mechanisms, as

previously suggested for other suspension-feeding species co-occurring with oysters (Dubois

and Colombo 2014). Indeed, *A. coerulea* medusae are cruising predators, capturing their prey

using locally generated flow currents (Dabiri et al. 2005) and the scyphistomae use a passive

ambush strategy (Huang et al. 2015), contrasting with the true filter-feeding strategy of the

oysters (Dubois et al. 2007; Dubois and Colombo 2014). The different mechanisms to capture

prey, likely promoted the selection and ingestion of different organic matter sources, reducing

the trophic competition for the same type of prey. Phytoplankton (especially diatoms) is the

main source of food for oysters (Dupuy et al. 2000; Pernet et al. 2012). In situ feeding

experiments showed that the consumption of *Aurelia* sp. medusae on micro- and

mesozooplankton organisms released the predation pressure from these secondary producers

on the lower trophic levels, boosting phytoplankton biomass and bacterial production (Turk et

al. 2008). Therefore, it is possible that the blooms of *A. coerulea* medusae might even be

advantageous for the production of oysters in the lagoon, via a top-down cascade effect on the

microbial community.

Bottom-up control of the A. coerulea population dynamics

In the Thau lagoon, the winter and early spring are critical periods for the formation of

the *A. coerulea* bloom (Marques et al. 2019). The production of ephyrae occurs between

657 November and April, with two main peaks: in November (during period 3) due to a high

658 percentage of the scyphistomae strobilating (despite their low densities), and in February –

659 March (during period 1), when this percentage is low but the density of scyphistomae is high

660 (Marques et al. 2019). As they grow to become medusae, the magnitude of the bloom is thus,

661 tightly dependent on the accumulated production of ephyrae, their survival, and growth rate.

662 In period 1, phytoplankton and microzooplankton are the main sources of food for both the

663 ephyrae and scyphistomae of *A. coerulea*. This stresses the role of the lower trophic levels in

664 the formation of the local jellyfish blooms: they promote higher levels of scyphistomae and

665 ephyrae survival and they boost the production of buds, leading to higher scyphistomae

666 densities and ephyrae production. In summer (during period 2) both *A. coerulea* life stages

667 change their diet to a mix of all sources (except small plankton for medusae). This is

668 particularly important because it supports the peak of the bloom, following high growth rates

669 of medusae, as well as their sexual reproduction (Fig. 11; Marques et al. 2015b). It is also

670 during this period that scyphistomae coverage declines (Fig. 11, Marques et al. 2019). Our

671 results suggest a potentially high intraspecific trophic competition between scyphistomae and

672 medusae, especially during this period. Therefore, the high abundance and high predation

673 pressure of the medusae might lead to the reduction of food availability for scyphistomae and

674 could contribute to the reduction of their coverage. During the following dry season (i.e.,

675 period 3), a bacteria-based food web prevails in the lagoon, with internal regeneration of

676 nitrogen, due to the absence of terrestrial freshwater inputs in the lagoon (Chapelle et al.

677 2000). This likely supports the peaks of microzooplankton abundance since these organisms

678 are recognized as important bacterivorous (Rassoulzadegan and Sheldon 1986).

679 Microzooplankton appear to have a critical role as a source of food for scyphistomae, which,

680 in period 3, would sustain not only the noticed peak of buds production in September but also

681   the main strobilation period in November (Marques et al. 2019), i.e., the first peak of ephyrae

682   production and the initial foundation of the subsequent jellyfish bloom in the Thau lagoon.

683

684   *Limitation of the study*

685   Although stable isotope analysis is a powerful tool to assess the trophic ecology of predators,

686   the MixSIAR results should be considered with caution. Indeed, mixing models always

687   provide a solution but their results might not always be biologically relevant: their precision

688   decreases with the number of introduced organic matter sources and depends greatly on the

689   accuracy of their signatures (Dubois et al. 2007).

690   In this work, we used a turnover time of one month for both jellyfish life stages, following the

691   results reported for *Aurelia* sp. (18 – 20 days, D'Ambra et al. 2014). If inaccurate, this might

692   have significantly biased the MixSIAR results for each isotopic niche period because the set

693   of organic matter source signatures matching with those of the jellyfish might be incorrect.

694   Moreover, despite the frequency of sampling for organic matter sources during our study,

695   some periods of the year (e.g. July – September) were less represented in the database. Given

696   the intra-annual variability in the isotopic signatures of the plankton component, we cannot

697   fully exclude that this sampling gap slightly biased our results.

698   The implementation of different isotopic fractionation values in the mixing models also

699   drastically modify their final results. In our study, using the fractionation values proposed by

700   D'Ambra et al. (2014) would result in a higher contribution of mesozooplankton to the diet in

701   both stages of *A. coerulea*. However, the values from D'Ambra et al. (2014) are very different

702   from those typically reported in the literature (e.g. Vander Zanden and Rasmussen 2001; Post

703   2002), leading to unrealistic trophic levels (Fleming et al. 2015; Milisenda et al. 2018).

704   Furthermore, the temperature (which is highly variable in Thau), the feeding condition, the

705 sexual maturity (e.g. Barnes et al. 2007), and, probably, the life stage might also affect

706 fractionation and turnover values.

707

708 **Conclusion**

709   Knowledge of the trophic ecology and population dynamics of jellyfish is imperative

710 to understand the main environmental drivers of blooms. With this regard, the Thau lagoon

711 offered an exceptional framework to study both benthic and pelagic trophic interactions and to

712 uncover the main organic matter sources supporting key periods of the *A. coerulea* life cycle.

713 In particular, we highlight the role of phytoplankton and microzooplankton in supporting

714 scyphistomae survival and asexual reproduction, that of mesozooplankton and sedimentary

715 organic matter for the growth of medusae, as well as the possible negative influence of

716 intraspecific competition on the benthic population dynamics. Moreover, we demonstrate that

717 the interspecific trophic competition between *A. coerulea* and the commonly cultivated oyster

718 *C. gigas* is likely to be limited, at least in the Thau lagoon, and therefore, we advocate that *A.*

719 *coerulea* blooms have a seemingly restricted impact on the local shellfish production.

720

721

722

723

724

725

726

References:

Anderson MJ (2017) Permutational Multivariate Analysis of Variance (PERMANOVA). In: Wiley StatsRef: Statistics Reference Online. John Wiley & Sons, Ltd, Chichester, UK, pp 1–15. doi: 10.1002/9781118445112.stat07841

Båmstedt U, Wild B, Martinussen MB (2001) Significance of food type for growth of ephyrae *Aurelia aurita* (Scyphozoa). Mar Biol 139:641–650. doi: 10.1007/s002270100623

Barnes C, Sweeting CJ, Jennings S, Barry JT, Polunin NVC (2007) Effect of temperature and ration size on carbon and nitrogen stable isotope trophic fractionation. Funct Ecol 21:356–362. doi: 10.1111/j.1365-2435.2006.01224.x

Boero F, Bouillon J, Gravili C, Miglietta MP, Parsons T, Piraino S (2008) Gelatinous plankton: irregularities rule the world (sometimes). Mar Ecol Prog Ser 356:299–310. doi: 10.3354/meps07368

Bonnet D, Molinero J-C, Schohn T, Daly-Yahia MN (2012) Seasonal changes in the population dynamics of *Aurelia aurita* in Thau lagoon. Cah Biol Mar 53:343–347.

Boyer S, Bouvy M, Bonnet D (2013) What triggers *Acartia* species egg production in a Mediterranean lagoon? Estuar Coast Shelf Sci 117:125–135. doi: 10.1016/j.ecss.2012.11.006

Chapelle A, Ménesguen A, Deslous-Paoli J-M, Souchu P, Mazouni N, Vaquer A, Millet B (2000) Modelling nitrogen, primary production and oxygen in a Mediterranean lagoon. Impact of oysters farming and inputs from the watershed. Ecol Modell 127:161–181. doi: 10.1016/S0304-3800(99)00206-9

Condon RH, Graham WM, Duarte CM, Pitt KA, Lucas CH, Haddock SHD, Sutherland KR, Robinson KL, Dawson MN, Decker MB, Mills CE, Purcell JE, Malej A, Mianzan H, Uye S-I, Gelcich S, Madin LP (2012) Questioning the Rise of Gelatinous Zooplankton in the World's Oceans. Bioscience 62:160–169. doi: 10.1525/bio.2012.62.2.9

752   D'Ambra I, Graham WM, Carmichael RH, Malej A, Onofri V (2013) Predation patterns and

753   prey quality of medusae in a semi-enclosed marine lake: implications for food web

754   energy transfer in coastal marine ecosystems. J Plankton Res 35:1305–1312. doi:

755   10.1093/plankt/fbt065

756   D'Ambra I, Carmichael RH, Graham WM (2014) Determination of $\delta^{13}C$ and $\delta^{15}N$ and trophic

757   fractionation in jellyfish: Implications for food web ecology. Mar Biol 161:473–480. doi:

758   10.1007/s00227-013-2345-y

759   Dabiri JO, Colin SP, Costello JH, Gharib M (2005) Flow patterns generated by oblate

760   medusan jellyfish: field measurements and laboratory analyses. J Exp Biol 208:1257 LP

761   – 1265. doi: 10.1242/jeb.01519

762   Dawson MN, Martin DL (2001) Geographic variation and ecological adaptation in *Aurelia*

763   *aurita* (Scyphozoa, Semaestomeae): some implications from molecular phylogenetics.

764   Hydrobiologia 451:259–273. doi: https://doi.org/10.1023/A:1011869215330

765   Dierking J, Morat F, Letourneur Y, Harmelin-Vivien M (2012) Fingerprints of lagoonal life:

766   Migration of the marine flatfish *Solea solea* assessed by stable isotopes and otolith

767   microchemistry. Estuar Coast Shelf Sci 104–105:23–32. doi: 10.1016/j.ecss.2011.03.018

768   Dubois S, Orvain F, Marin-Léal JC, Ropert M, Lefebvre S (2007) Small-scale spatial

769   variability of food partitioning between cultivated oysters and associated suspension-

770   feeding species, as revealed by stable isotopes. Mar Ecol Prog Ser 336:151–160. doi:

771   10.3354/meps336151

772   Dubois SF, Colombo F (2014) How picky can you be? Temporal variations in trophic niches

773   of co-occurring suspension-feeding species. Food Webs 1:1–9. doi:

774   10.1016/j.fooweb.2014.07.001

775   Dupuy C, Vaquer A, Lam-Höai T, Rougier C, Mazouni N, Lautier J, Collos Y, Le Gall S

776   (2000) Feeding rate of the oyster *Crassostrea gigas* in a natural planktonic community of

777   the Mediterranean Thau Lagoon. Mar Ecol Prog Ser 205:171–184. doi:

778   10.3354/meps205171

779 Escalas A, Ferraton F, Paillon C, Vidy G, Carcaillet F, Salen-Picard C, Le Loc'h F, Richard

780   P, Darnaude AM (2015) Spatial variations in dietary organic matter sources modulate the

781   size and condition of fish juveniles in temperate lagoon nursery sites. Estuar Coast Shelf

782   Sci 152:78–90. doi: 10.1016/j.ecss.2014.11.021

783 Fleming NEC, Harrod C, Newton J, Houghton JDR (2015) Not all jellyfish are equal: isotopic

784   evidence for inter- and intraspecific variation in jellyfish trophic ecology. PeerJ 3:e1110.

785   doi: 10.7717/peerj.1110

786 Fouilland E, Trottet A, Bancon-Montigny C, Bouvy M, Le Floc'h E, Gonzalez J-L, Hatey E,

787   Mas S, Mostajir B, Nouguier J, Pecqueur D, Rochelle-Newall E, Rodier C, Roques C,

788   Salles C, Tournoud M-G, Vidussi F (2012) Impact of a river flash flood on microbial

789   carbon and nitrogen production in a Mediterranean Lagoon (Thau Lagoon, France).

790   Estuar Coast Shelf Sci 113:192–204. doi: 10.1016/j.ecss.2012.08.004

791 Frazer TK, Ross RM, Quetin LB, Montoya JP (1997) Turnover of carbon and nitrogen during

792   growth of larval krill, *Euphausia superba* Dana: a stable isotope approach. J Exp Mar

793   Bio Ecol 212:259–275. doi: 10.1016/S0022-0981(96)02740-2

794 Han C-H, Uye S-I (2010) Combined effects of food supply and temperature on asexual

795   reproduction and somatic growth of polyps of the common jellyfish *Aurelia aurita* s.l.

796   Plankt Benthos Res 5:98–105. doi: 10.3800/pbr.5.98

797 Hansson LJ (2006) A method for in situ estimation of prey selectivity and predation rate in

798   large plankton, exemplified with the jellyfish *Aurelia aurita* (L.). J Exp Mar Bio Ecol

799   328:113–126. doi: 10.1016/j.jembe.2005.07.002

800 Huang XG, Huang B, Zeng Y, Li SX (2015) Effect of dinoflagellates and diatoms on the

801   feeding response and survival of *Aurelia* sp. polyps. Hydrobiologia 754:179–188. doi:

802   10.1007/s10750-014-2023-1

803   Hubot N, Lucas CH, Piraino S (2017) Environmental control of asexual reproduction and

804   somatic growth of *Aurelia* spp. (Cnidaria, Scyphozoa) polyps from the Adriatic Sea.

805   PLoS One 12:e0178482. doi: 10.1371/journal.pone.0178482

806   Ikeda H, Mizota C, Uye S-I (2017) Bioenergetic characterization in *Aurelia aurita* (Cnidaria:

807   Scyphozoa) polyps and application to natural polyp populations. Mar Ecol Prog Ser

808   568:87–100. doi: 10.3354/meps12055

809   Ishii H, Båmstedt U (1998) Food regulation of growth and maturation in a natural population

810   of *Aurelia aurita* (L.). J Plankton Res 20:805–816. doi: 10.1093/plankt/20.5.805

811   Ishii H, Tanaka F (2001) Food and feeding of *Aurelia aurita* in Tokyo Bay with an analysis of

812   stomach contents and a measurement of digestion times. In: Purcell JE, Graham WM,

813   Dumont HJ (eds) Jellyfish Blooms: Ecological and Societal Importance. Developments

814   in Hydrobiology, vol 155, Springer Netherlands, Dordrecht, pp 311–320. doi:

815   10.1007/978-94-010-0722-1_26

816   Jackson AL, Inger R, Parnell AC, Bearhop S (2011) Comparing isotopic niche widths among

817   and within communities: SIBER - Stable Isotope Bayesian Ellipses in R. J Anim Ecol

818   80:595–602. doi: 10.1111/j.1365-2656.2011.01806.x

819   Jaine AK (2010) Data clustering: 50 years beyond K-means Pattern Recognit Lett 31:651-

820   666. 10.1016/j.patrec.2009.09.011.

821   Javidpour J, Cipriano-Maack AN, Mittermayr A, Dierking J (2016) Temporal dietary shift in

822   jellyfish revealed by stable isotope analysis. Mar Biol 163:112. doi: 10.1007/s00227-

823   016-2892-0

824   Kamiyama T (2013) Planktonic ciliates as food for the scyphozoan *Aurelia aurita* (s.l.):

825   Effects on asexual reproduction of the polyp stage. J Exp Mar Bio Ecol 445:21–28. doi:

826   10.1016/j.jembe.2013.03.018

827   Kassambara A, Mundt F (2017) factoextra: Extract and Visualize the Results of Multivariate

828   Data Analyses. 1–74. R package version 1.0.5

829   Layman CA, Araujo MS, Boucek R, Hammerschlag-Peyer CM, Harrison E, Jud ZR, Matich

830   P, Rosenblatt AE, Vaudo JJ, Yeager LA, Post DM, Bearhop S (2012) Applying stable

831   isotopes to examine food-web structure: an overview of analytical tools. Biol Rev

832   87:545–562. doi: 10.1111/j.1469-185X.2011.00208.x

833   Lo WT, Chen IL (2008) Population succession and feeding of scyphomedusae, *Aurelia aurita*,

834   in a eutrophic tropical lagoon in Taiwan. Estuar Coast Shelf Sci 76:227–238. doi:

835   10.1016/j.ecss.2007.07.015

836   Lucas CH (1994) Biochemical composition of *Aurelia aurita* in relation to age and sexual

837   maturity. J Exp Mar Bio Ecol 183:179–192. doi: 10.1016/0022-0981(94)90086-8

838   Lucas CH (2001) Reproduction and life history strategies of the common jellyfish, *Aurelia*

839   *aurita*, in relation to its ambient environment. In: Purcell JE, Graham WM, Dumont HJ

840   (eds) Jellyfish Blooms: Ecological and Societal Importance. Developments in

841   Hydrobiology, vol 155, Springer Netherlands, Dordrecht, pp 229–246doi: 10.1007/978-

842   94-010-0722-1_19

843   Lucas CH, Hirst AG, Williams JA (1997) Plankton Dynamics and *Aurelia aurita* Production

844   in Two Contrasting Ecosystems: Comparisons and Consequences. Estuar Coast Shelf Sci

845   45:209–219. doi: 10.1006/ecss.1996.0173

846   Marques R, Cantou M, Soriano S, Molinero J-C, Bonnet D (2015a) Mapping distribution and

847   habitats of *Aurelia* sp. polyps in Thau lagoon, north-western Mediterranean sea (France).

848   Mar Biol 162:1441–1449. doi: 10.1007/s00227-015-2680-2

849   Marques R, Albouy-Boyer S, Delpy F, Carré C, Le Floc'H É, Roques C, Molinero J-C,

850   Bonnet D (2015b) Pelagic population dynamics of *Aurelia* sp. in French Mediterranean

851   lagoons. J Plankton Res 37:1019–1035. doi: 10.1093/plankt/fbv059

852   Marques R, Darnaude AM, Schiariti A, Tremblay Y, Molinero J-C, Soriano S, Hatey E,

853   Colantoni S, Bonnet D (2019) Dynamics and asexual reproduction of the jellyfish

854   *Aurelia coerulea* benthic life stage in the Thau lagoon (northwestern Mediterranean).

855   Mar Biol 166:74. doi: 10.1007/s00227-019-3522-4

856   Martinez Arbizu P (2019) pairwiseAdonis: Pairwise multilevel comparison using adonis. R

857   package, version 0.0.1.

858   Martinussen MB, Båmstedt U (2001) Digestion rate in relation to temperature of two

859   gelatinous planktonic predators. Sarsia 86:21–35. doi:

860   10.1080/00364827.2001.10420458

861   Milisenda G, Rossi S, Vizzini S, Fuentes VL, Purcell JE, Tilves U, Piraino S (2018) Seasonal

862   variability of diet and trophic level of the gelatinous predator *Pelagia noctiluca*

863   (Scyphozoa). Sci Rep 8:12140. doi: 10.1038/s41598-018-30474-x

864   Millet B, Cecchi P (1992) Wind-induced hydrodynamic control of the phytoplankton biomass

865   in a lagoon ecosystem. Limnol Oceanogr 37:140–146. doi: 10.4319/lo.1992.37.1.0140

866   Mills C (2001) Are population increasing globally in response to changing ocean conditions?

867   Hydrobiologia 451:55–68. doi: https://doi.org/10.1023/A:1011888006302

868   Mongruel R, Vanhoutte-Brunier A, Fiandrino A, Valette F, Ballé-Béganton J, Pérez Agúndez

869   JA, Gallai N, Derolez V, Roussel S, Lample M, Laugier T (2013) Why, how, and how

870   far should microbiological contamination in a coastal zone be mitigated? An application

871   of the systems approach to the Thau lagoon (France). J Environ Manage 118:55–71. doi:

872   10.1016/j.jenvman.2012.12.038

873   Morais P, Dias E, Cruz J, Chainho P, Angélico MM, Costa JL, Barbosa AB, Teodósio MA

874   (2017) Allochthonous-derived organic matter subsidizes the food sources of estuarine

875   jellyfish. J Plankton Res 39:870–877. doi: 10.1093/plankt/fbx049

876   Nixon SW (1995) Coastal marine eutrophication: A definition, social causes, and future

877 concerns. Ophelia 41:199–219. doi: 10.1080/00785236.1995.10422044

878 Oksanen J, Blanchet FG, Friendly M, Kindt R, Legendre P, Mcglinn D, Minchin PR, O'Hara

879   RB, Simpson GL, Solymos P, Stevens MHH, Szoecs E, Wagner H (2019) Vegan:

880   Community Ecology Package. R package, version 2.5-4

881 Östman C (1997) Abundance, feeding behaviour and nematocysts of scyphopolyps (Cnidaria)

882   and nematocysts in their predator, the nudibranch *Coryphella verrucosa* (Mollusca). In:

883   Naumov AD, Hummel H, Sukhotin AA, Ryland JS (eds) Interactions and Adaptation

884   Strategies of Marine Organisms. Springer Netherlands, Dordrecht, pp 21–28

885 Pernet F, Malet N, Pastoureaud A, Vaquer A, Quéré C, Dubroca L (2012) Marine diatoms

886   sustain growth of bivalves in a Mediterranean lagoon. J Sea Res 68:20–32. doi:

887   10.1016/j.seares.2011.11.004

888 Perrin J-L, Tournoud M-G (2009) Hydrological processes controlling flow generation in a

889   small Mediterranean catchment under karstic influence. Hydrol Sci J 54:1125–1140. doi:

890   10.1623/hysj.54.6.1125

891 Pinnegar JK, Polunin NVC (1999) Differential fractionation of $\delta^{13}C$ and $\delta^{15}N$ among fish

892   tissues: implications for the study of trophic interactions. Funct Ecol 13:225–231. doi:

893   10.1046/j.1365-2435.1999.00301.x

894 Pitt KA, Connolly RM, Meziane T (2009) Stable isotope and fatty acid tracers in energy and

895   nutrient studies of jellyfish: A review. Hydrobiologia 616:119–132. doi:

896   10.1007/s10750-008-9581-z

897 Plus M, La Jeunesse I, Bouraoui F, Zaldívar J-M, Chapelle A, Lazure P (2006) Modelling

898   water discharges and nitrogen inputs into a Mediterranean lagoon: Impact on the primary

899   production. Ecological Modelling 193:69–89. doi:10.1016/j.ecolmodel.2005.07.037

900 Post DM (2002) Using stable isotopes to estimate trophic position: models, methos, and

901   assumptions. . Ecology 83:703–718. doi: Doi 10.2307/3071875

902 Post DM, Layman CA, Arrington DA, Takimoto G, Quattrochi J, Montaña CG (2007) Getting

903 to the fat of the matter: Models, methods and assumptions for dealing with lipids in

904 stable isotope analyses. Oecologia 152:179–189. doi: 10.1007/s00442-006-0630-x

905 Purcell JE (2012) Jellyfish and Ctenophore Blooms Coincide with Human Proliferations and

906 Environmental Perturbations. Ann Rev Mar Sci 4:209–235. doi: 10.1146/annurev-

907 marine-120709-142751

908 Rassoulzadegan F, Sheldon RW (1986) Predator-prey interactions of nanozooplankton and

909 bacteria in an oligotrophic marine environment. Limnol Oceanogr 31:1010–1029. doi:

910 10.4319/lo.1986.31.5.1010

911 Stock BC, Semmens BX (2016) MixSIAR GUI User Manual. Version 3.1 1–42. doi:

912 10.5281/zenodo.47719

913 Syväranta J, Rautio M (2010) Zooplankton, lipids and stable isotopes: importance of seasonal,

914 latitudinal, and taxonomic differences. Can J Fish Aquat Sci 67:1721–1729. doi:

915 10.1139/F10-091

916 Turk V, Lučić D, Flander-Putrle V, Malej A (2008) Feeding of *Aurelia* sp. (Scyphozoa) and

917 links to the microbial food web. Mar Ecol 29:495–505. doi: 10.1111/j.1439-

918 0485.2008.00250.x

919 Utermöhl H (1958) Zur Vervollkommnung der quantitativen Phytoplankton-Methodik. SIL

920 Commun 1953-1996 9:1–38. doi: 10.1080/05384680.1958.11904091

921 Wang Y-T, Zheng S, Sun S, Zhang F (2015) Effect of temperature and food type on asexual

922 reproduction in *Aurelia* sp.1 polyps. Hydrobiologia 754:169–178. doi: 10.1007/s10750-

923 014-2020-4

924 Yokoyama H, Tamaki A, Harada K, Shimoda K, Koyama K, Ishihi Y (2005) Variability of

925 diet-tissue isotopic fractionation in estuarine macrobenthos. Mar Ecol Prog Ser 296:115–

926 128. doi: 10.3354/meps296115

927   Vander Zanden MJ, Rasmussen JB (2001) Variation in δ^{15}N and δ^{13}C trophic fractionation:

928   Implications for aquatic food web studies. Limnol Oceanogr 46:2061–2066. doi:

929   10.4319/lo.2001.46.8.2061

930   Zheng S, Sun X, Wang Y, Sun S (2015) Significance of different microalgal species for

931   growth of moon jellyfish ephyrae, *Aurelia* sp.1. J Ocean Univ China 14:823–828. doi:

932   10.1007/s11802-015-2775-x

933   Zuur AF, Ieno EN, Walker NJ, Saveliev AA, Smith GM (2009) Mixed Effects Models and

934   Extensions in Ecology with R. Springer New York

935

936

937

938

939

Tables

953 Table 1: Frequency of occurrence (FO), index of relative importance (IRI) and mean

954 abundance of prey items found in *A. coerulea* medusae gut contents during the period of its

955 presence in the Thau lagoon. Numbers in parenthesis are the number of medusae with prey

956 items analyzed.

Prey	FO (%)			IRI (%)			Abundance (± SD) (ind.medusae^{-1})		
	Apr (5)	May (9)	Jun (8)	Apr (5)	May (9)	Jun (8)	Apr (5)	May (9)	Jun (8)
Phytoplankton	20.0	33.3	0.0	3.4	5.6	0.0	1.0 (2.2)	1.0 (1.8)	0.0 (0.0)
Microzooplankton	60.0	55.6	0.0	7.5	12.5	0.0	2.2 (3.8)	2.2 (3.4)	0.0 (0.0)
Mesozooplankton (total)	80.0	88.9	100	89.1	81.9	100	26.2 (35.4)	14.6 (13.4)	10.3 (18.3)
- Copepods	40.0	66.7	87.5	34.7	21.9	46.3	10.2 (20.1)	3.9 (5.7)	4.8 (9.9)
- Nauplii (copepods and cirripeds)	60.0	88.9	62.5	4.8	31.3	41.5	1.4 (2.1)	5.6 (8.5)	4.3 (7.8)
- Other crustaceans	20.0	55.6	50.0	0.7	10.0	8.5	0.2 (0.4)	1.8 (3.5)	0.9 (1.1)
- Non-crustaceans	60.0	66.7	25.0	49.0	18.8	3.7	14.4 (20.9)	3.3 (4.5)	0.4 (0.7)

957

958

959 Table 2: Parameters of the generalized linear models used to assess correlations between the

960 benthic population dynamics variables (scyphistomae coverage and scyphistomae producing

961 buds) with the abundance [ln (x+1)] of phytoplankton (cell L^{-1}), microzooplankton (cell L^{-1})

962 and mesozooplankton (ind m^{-3}).

	Estimate	Std. Error	t value	p-value
Scyphistomae coverage (%)				
(Intercept)	-0.17	0.07	-2.46	0.03
Phytoplankton	0.02	0.01	2.97	**0.01**
Microzooplankton	0.01	0.01	2.10	0.05
Mesozooplankton	0.00	0.00	0.02	0.98
Scyphistomae producing buds (%)				
(Intercept)	-3.82	0.35	-10.95	**< 0.01**
Phytoplankton	-0.01	0.03	-0.47	0.64
Microzooplankton	0.26	0.03	10.19	**< 0.01**
Mesozooplankton	0.00	0.02	-0.09	0.93

963

964

965   Table 3: Stable δ^{13}C and δ^{15}N isotope signatures (mean ± SD) of *A. coerulea* and organic

966   matter sources used in MixSIAR model for each isotopic niche period. Sources A are the

967   values of organic matter sources used for scyphistomae models, including all data, while

968   Sources B are the values of organic matter sources collected from February to May, used for

969   medusae models. *n* is the number of samples used to calculate each mean. SP: small plankton;

970   Mesoz.: mesozooplankton; SOM: sedimentary organic matter.

	Period 1			Period 2			Period 3		
	δ^{13}C (± SD) ‰	δ^{15}N (± SD) ‰	*n*	δ^{13}C (± SD) ‰	δ^{15}N (± SD) ‰	*n*	δ^{13}C (± SD) ‰	δ^{15}N (± SD) ‰	*n*
Scyphistomae	-22.8 (0.4)	8.0 (0.5)	18	-19.3 (0.2)	9.0 (0.1)	9	-21.1 (0.3)	8.5 (0.4)	9
Medusae	-23.4 (0.7)	8.1 (0.3)	13	-19.4 (0.5)	8.9 (0.3)	7			
Sources A									
SP	-22.1 (2.0)	6.5 (0.3)	18	-20.6 (0.8)	6.2 (0.7)	22	-21.0 (0.9)	6.7 (0.3)	6
Mesoz.	-22.9 (0.9)	8.0 (0.4)	9	-19.2 (0.7)	7.4 (0.3)	12	-20.1 (0.1)	7.5 (0.0)	3
SOM	-20.2 (0.9)	5.5 (0.3)	6	-20.6 (0.1)	5.4 (0.2)	6	-20.7 (0.0)	5.3 (0.0)	2
Sources B									
SP	-23.3 (0.9)	6.4 (0.3)	12	-20.9 (0.5)	5.8 (0.3)	15			
Mesoz.	-23.4 (0.3)	8.2 (0.2)	6	-18.8 (0.2)	7.3 (0.3)	9			
SOM	-18.9 (0.0)	5.8 (0.1)	2	-20.5 (0.0)	5.6 (0.0)	2			

971

972

974
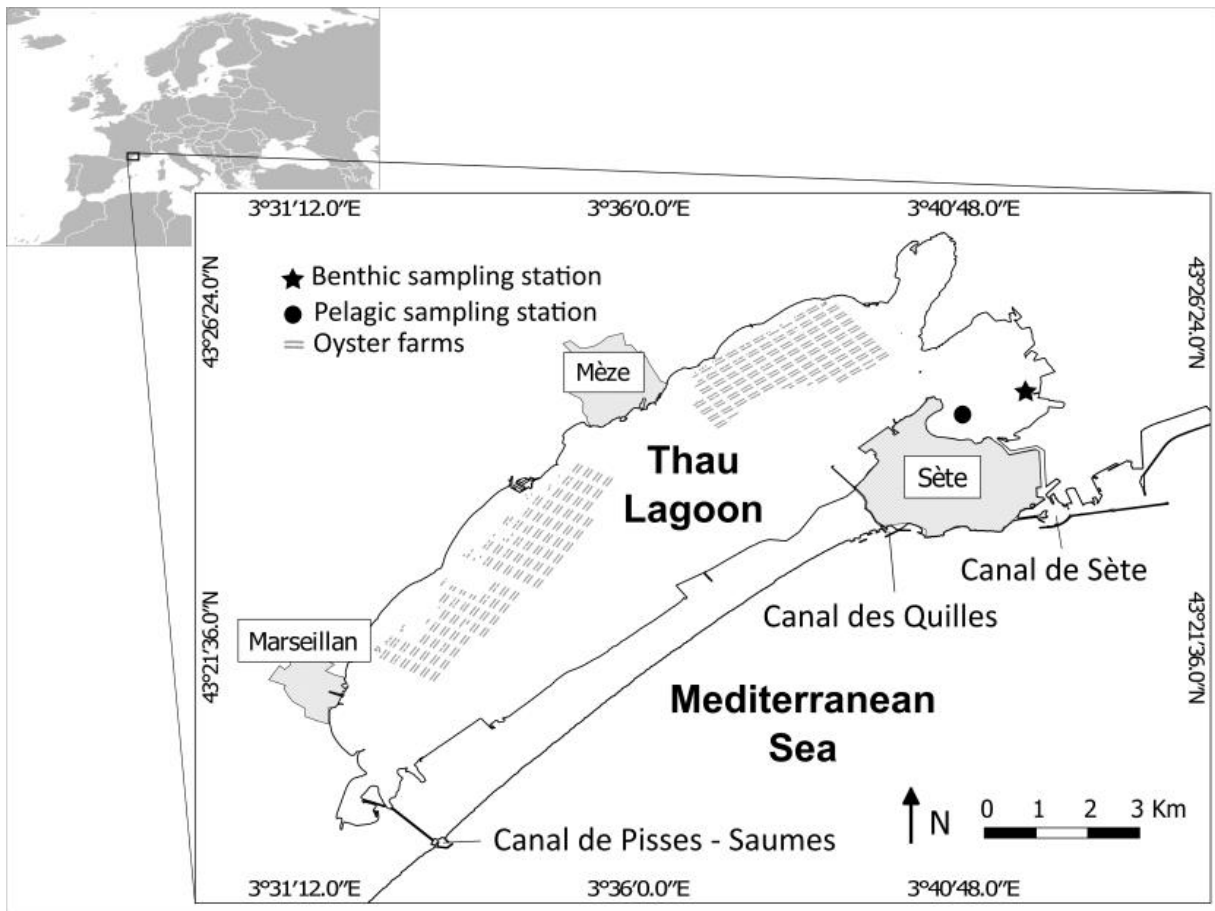
976 Fig. 1: Map of the Thau lagoon showing the location of the benthic (star) and pelagic (dot)

977 sampling stations for this study. Shaded areas represent urban zones and grey points represent

978 oyster farms.

979

44
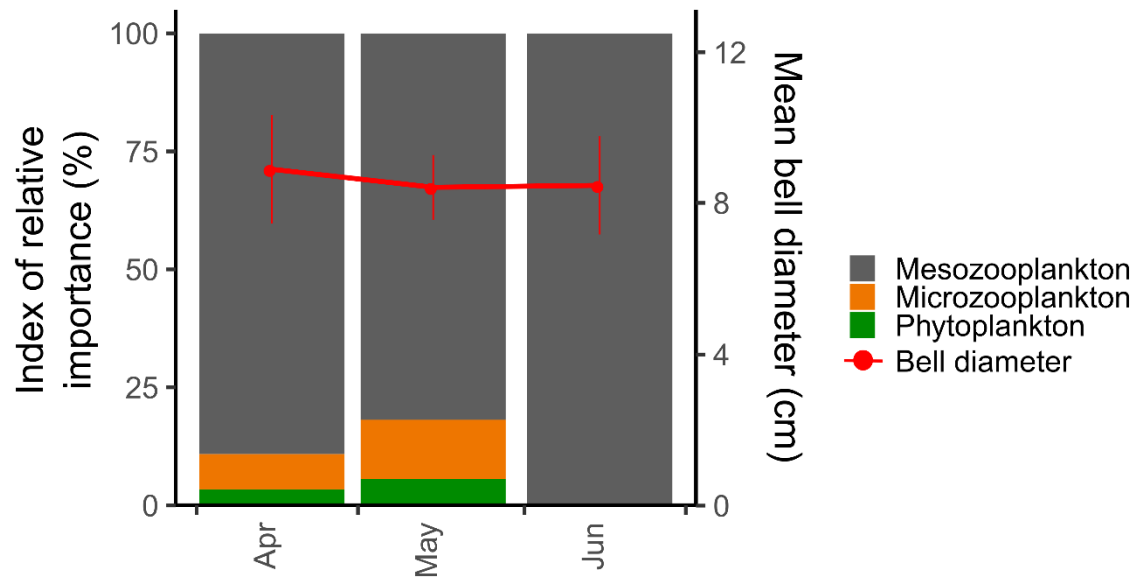
980

981   Fig. 2: Index of relative importance of the three main prey groups found in the guts of *A.*

982   *coerulea* medusae and the bell diameter of all individuals collected for gut content analysis.
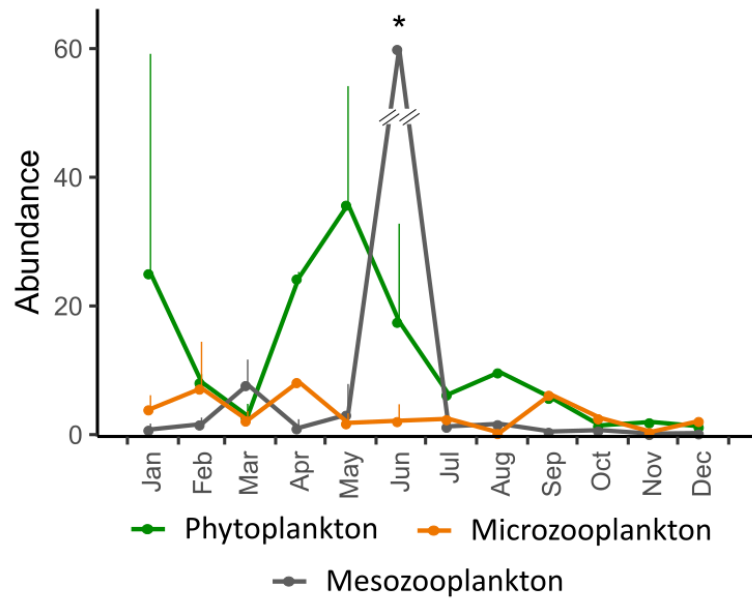
983

984

985

986

987

988

989

990

Fig. 3: Temporal variability of phytoplankton ($\times 10^3$ cell L^{-1}), microzooplankton ($\times 10^3$ cell L^{-1}), and mesozooplankton ($\times 10^3$ ind m^{-3}) abundance collected in the Thau lagoon during the study period. All values represent monthly mean $\pm$ SD. In June 2017 (*), the mean ($\pm$ SD) of mesozooplankton abundance was 90,895 $\pm$ 107,072 ind m^{-3}.

995

996

997

998

999
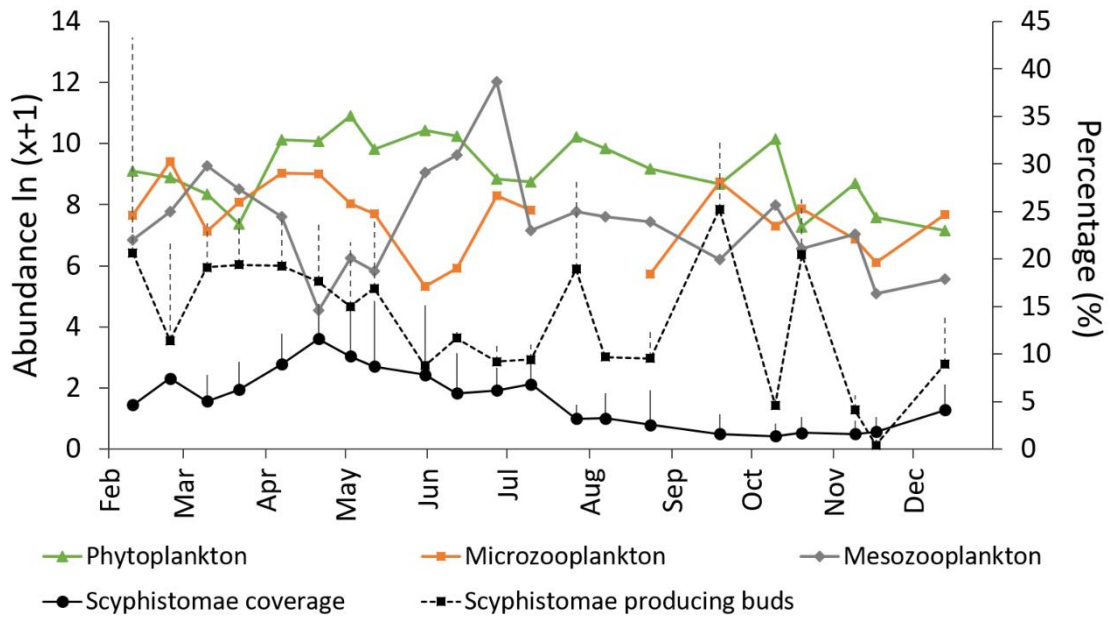
Fig. 4: Temporal variability of the *A. coerulea* benthic population dynamics and the abundance of plankton in the Thau lagoon during the study period (adapted from Marques et al. 2019). Black lines represent the percentage of scyphistomae coverage (i.e., an indicator of population size) and the percentage of the scyphistomae producing buds. Each point represents replicate means and vertical lines are SD (see Marques et al 2019 for further information). Coloured lines represent the non-averaged abundance (after logarithmic transformation) of phytoplankton (cell L^{-1}), microzooplankton (cell L^{-1}), and mesozooplankton (ind m^{-3}).
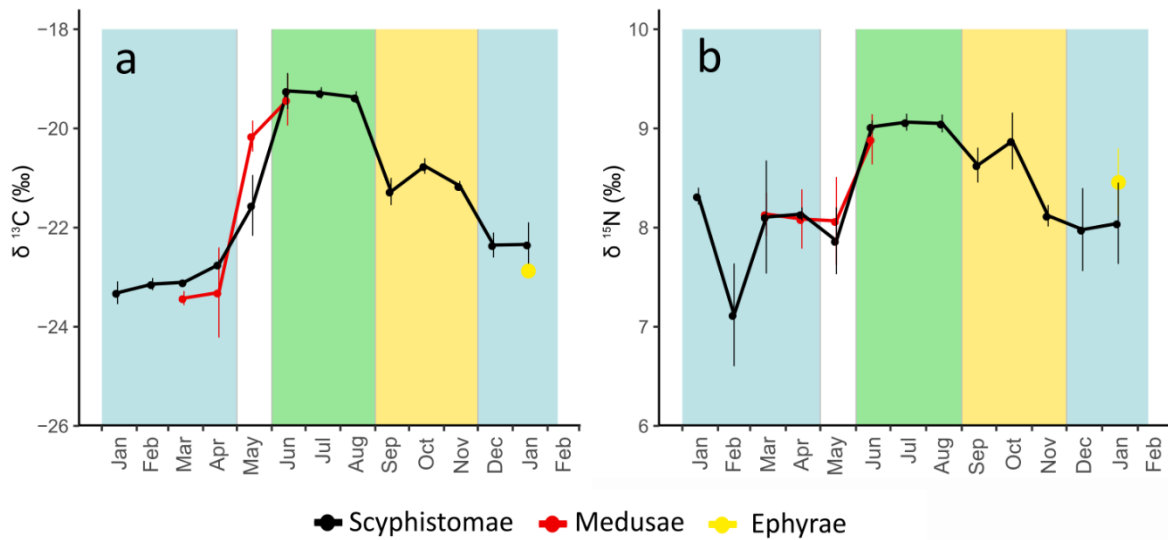
Fig. 5: Temporal variability of $\delta^{13}C$ (a) and $\delta^{15}N$ (b) of *A. coerulea* scyphistomae, medusae, and ephyrae in Thau. All values represent monthly means ± SD. Background colours represent the different isotopic niche periods (periods 1, 2, and 3 in blue, green, and yellow, respectively; see Fig.6). May represents a transitional period and it was not included in any isotopic niche period.
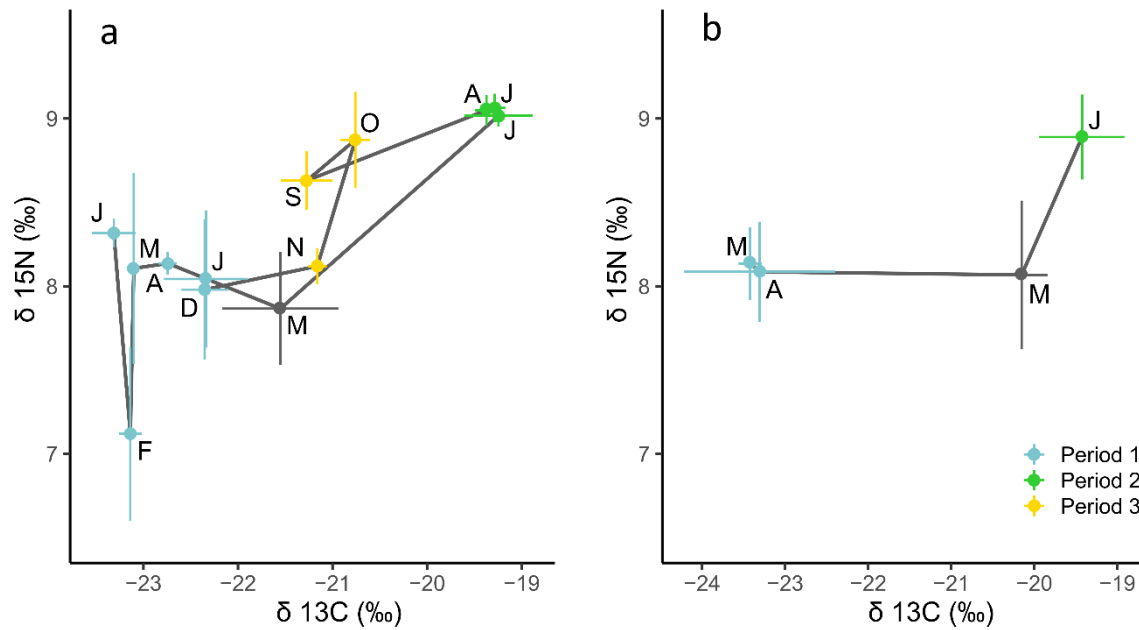
Fig. 6: Time trajectory of the evolution of the isotope signature, averaged by month, from *A. coerulea* scyphistomae (a) and medusae (b). Letters represent months (from January 2017 to January 2018). Coloured points represent isotopic niche periods defined after cluster analysis: period 1 is from January to April 2017 and from December 2017 to January 2018; period 2 is from June to August 2017 and period 3 is from September to November 2017. May represents the transition between periods 1 and 2 and was therefore not included in any isotopic niche period.
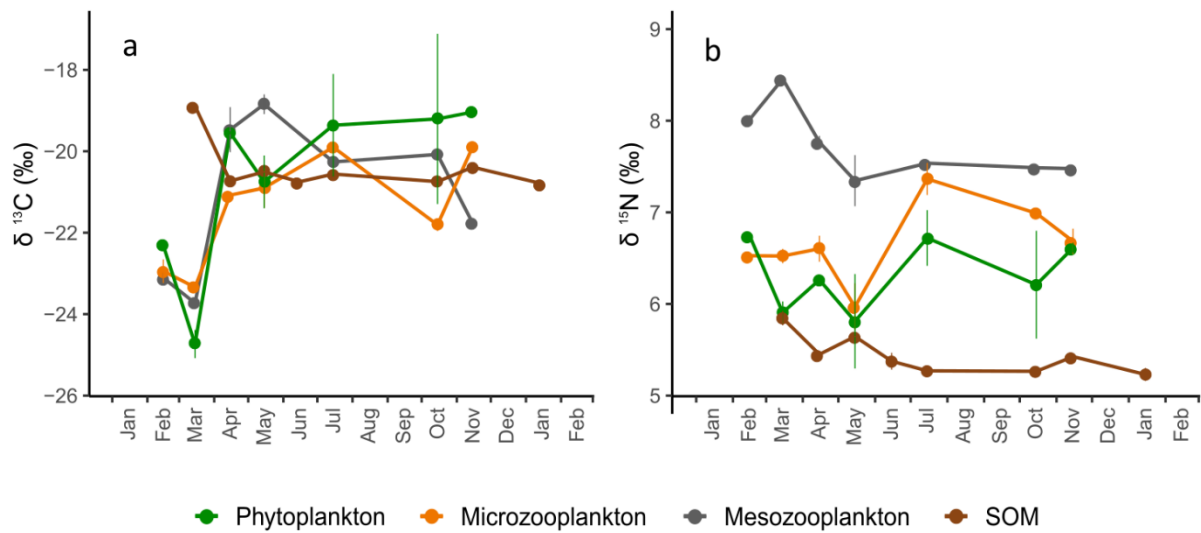
1032

1033   Fig. 7: Monthly variability of the $\delta^{13}C$ (a) and $\delta^{15}N$ (b) of the organic matter sources collected

1034   in this study. SOM: sedimentary organic matter.

1035

1036

1037

1038
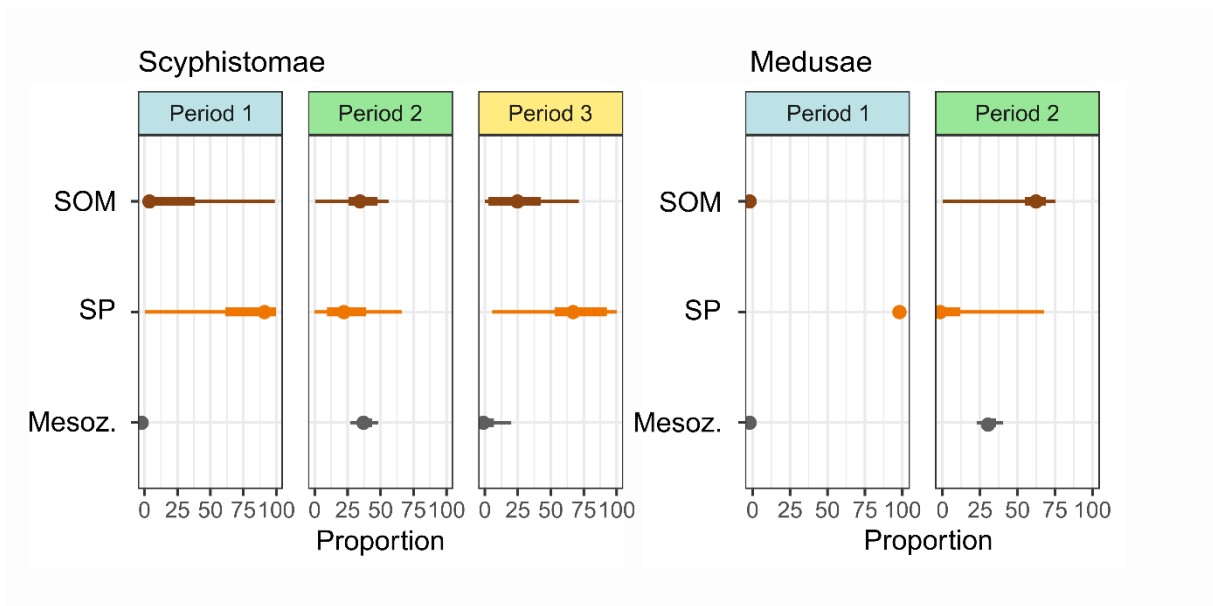
1039

1040

1041

1042

1043

Fig. 8: Proportion of the contribution of each organic matter source to the diet of *A. coerulea*

scyphistomae and medusae during the different isotopic niche periods. The proportion was

calculated using MixSIAR mixing models. The points indicate the median and the horizontal

bars represent 75% and 95% Bayesian credibility intervals. SOM: sedimentary organic matter,
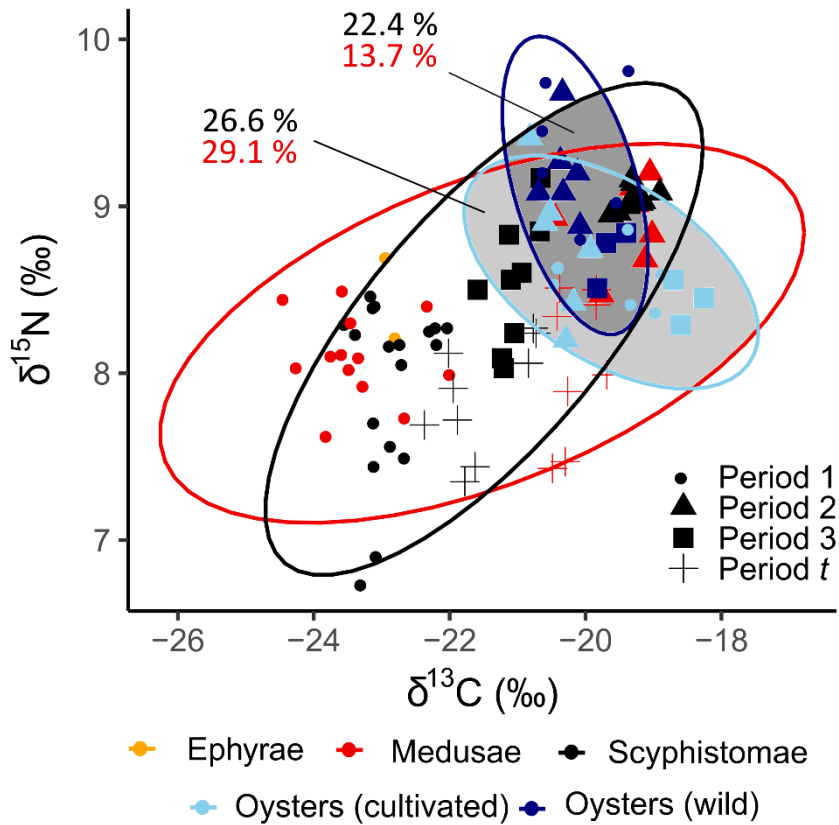
SP: small plankton, Mesoz.: mesozooplankton.
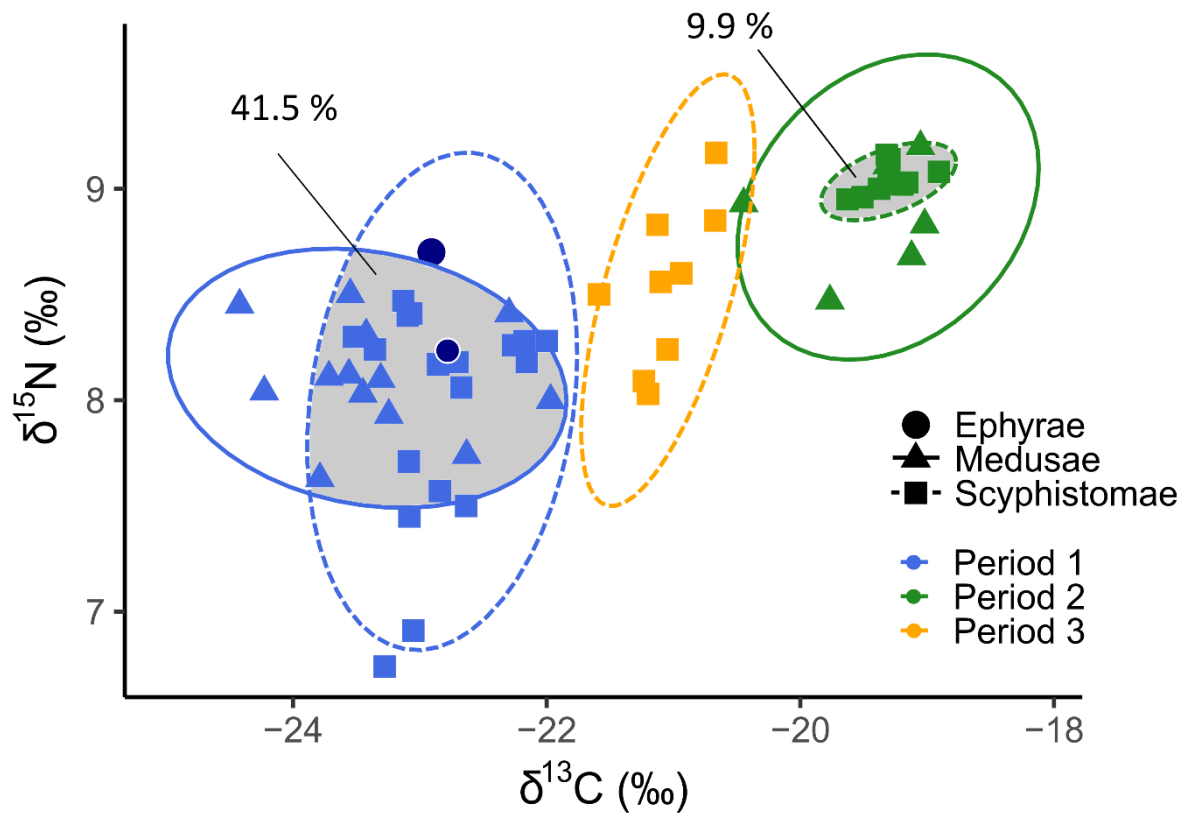
Fig. 9: Biplot of isotope values of *A. coerulea* ephyrae, medusae, and scyphistomae. Ellipses indicate their isotopic niche in the Thau lagoon (as 95% confidence ellipse of the bivariate means), during the different isotopic niche periods. Grey areas and associated values indicate the percentage of overlap, when observed.

Fig. 10: Biplot of isotope values of *A. coerulea* ephyrae, medusae, scyphistomae, and oysters
(*C. gigas*). Ellipses indicate their isotopic niche in the Thau lagoon, considering the whole
study period (as 95% confidence ellipse of the bivariate means). Dark and light grey areas
indicate niche overlap between *A. coerulea* and wild or cultivated oysters, respectively.
Associated values on the graph indicate the percentage of overlap with medusae (in red) and
scyphistomae (in black). The shape of points represents isotopic niche periods (period *t*:
transitional period, i.e., samples collected in May).
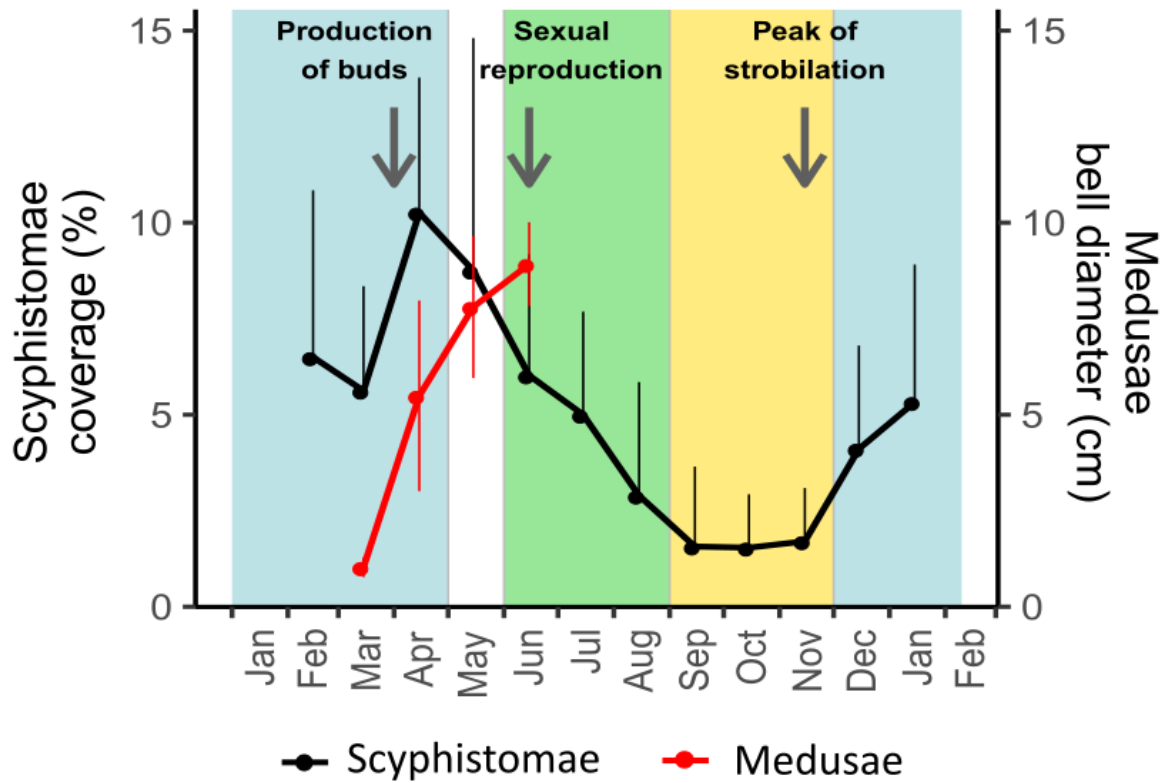
Fig. 6: Scyphistomae coverage (in black, from Marques et al. 2019) and medusae bell diameter of the individuals collected for stable isotope analysis in this study (in red). The arrows indicate the main periods of sexual and asexual reproduction of *A. coerulea* (after Marques et al. 2015b, 2019). The background colours represent the isotopic niche periods (periods 1, 2, and 3 in blue, green, and yellow, respectively).